



NAVAL POSTGRADUATE SCHOOL

MONTEREY, CALIFORNIA

THESIS

DESIGN OF A COAXIAL SPLIT FLOW PULSE DETONATION ENGINE

by

Philip D. Hall

June 2006

Thesis Advisor:
Second Reader:

Jose O. Sinibaldi
Christopher M. Brophy

Approved for public release; distribution is unlimited

THIS PAGE INTENTIONALLY LEFT BLANK

| | | | | |
|--|---|--|--|--|
| REPORT DOCUMENTATION PAGE | | | <i>Form Approved OMB No. 0704-0188</i> | |
| Public reporting burden for this collection of information is estimated to average 1 hour per response, including the time for reviewing instruction, searching existing data sources, gathering and maintaining the data needed, and completing and reviewing the collection of information. Send comments regarding this burden estimate or any other aspect of this collection of information, including suggestions for reducing this burden, to Washington headquarters Services, Directorate for Information Operations and Reports, 1215 Jefferson Davis Highway, Suite 1204, Arlington, VA 22202-4302, and to the Office of Management and Budget, Paperwork Reduction Project (0704-0188) Washington DC 20503. | | | | |
| 1. AGENCY USE ONLY (Leave blank) | | 2. REPORT DATE June 2006 | 3. REPORT TYPE AND DATES COVERED Master's Thesis | |
| 4. TITLE AND SUBTITLE: Design of a Coaxial Split Flow Pulse Detonation Engine | | | 5. FUNDING NUMBERS | |
| 6. AUTHOR(S) Philip D. Hall | | | | |
| 7. PERFORMING ORGANIZATION NAME(S) AND ADDRESS(ES) Naval Postgraduate School Monterey, CA 93943-5000 | | | 8. PERFORMING ORGANIZATION REPORT NUMBER | |
| 9. SPONSORING /MONITORING AGENCY NAME(S) AND ADDRESS(ES) | | | 10. SPONSORING/MONITORING AGENCY REPORT NUMBER | |
| 11. SUPPLEMENTARY NOTES The views expressed in this thesis are those of the author and do not reflect the official policy or position of the Department of Defense or the U.S. Government. | | | | |
| 12a. DISTRIBUTION / AVAILABILITY STATEMENT Approved for public release; distribution is unlimited | | | 12b. DISTRIBUTION CODE | |
| 13. ABSTRACT (maximum 200 words) <p>Future Navy Capabilities indicate the need for a supersonic cruise missile. Thus the need exists for a low cost, light-weight, and efficient means of supersonic propulsion. NPS has been developing the Pulse Detonation Engine, which in theory has a thermodynamic efficiency greater than 50% as compared to 35% for state of the art constant-pressure cycles currently in use in gas turbines/ramjets/scramjets. Nonetheless, there are two major problems in the development of this engine. These are the increase of the propulsive efficiency by removing the oxygen-assisted initiator currently in use, and the reduction of internal total pressure losses caused by the highly constrictive internal flow-path geometry currently required to promote the deflagration to detonation transition (DDT). The aforementioned problems have been addressed and a viable design proposed through the implementation of a novel Transient Plasma Ignition system and a split-flow path engine geometry as described in this work. Future work will concentrate on the development of a performance measurement test rig to experimentally assess the designs presented herein.</p> | | | | |
| 14. SUBJECT TERMS Pulse Detonation Engines, PDE, PDE Ignition, Transient Plasma Ignition, TPI, Coaxial Split Flow | | | 15. NUMBER OF PAGES 59 | |
| | | | 16. PRICE CODE | |
| 17. SECURITY CLASSIFICATION OF REPORT Unclassified | 18. SECURITY CLASSIFICATION OF THIS PAGE Unclassified | 19. SECURITY CLASSIFICATION OF ABSTRACT Unclassified | 20. LIMITATION OF ABSTRACT UL | |

THIS PAGE INTENTIONALLY LEFT BLANK

Approved for public release; distribution is unlimited

DESIGN OF A COAXIAL SPLIT FLOW PULSE DETONATION ENGINE

Philip D. Hall
Ensign, United States Navy
B.S., United States Naval Academy, 2005

Submitted in partial fulfillment of the
requirements for the degree of

MASTER OF SCIENCE IN MECHANICAL ENGINEERING

from the

**NAVAL POSTGRADUATE SCHOOL
June 2006**

Author: Philip D. Hall

Approved by: Jose O. Sinibaldi
Thesis Advisor

Christopher M. Brophy
Co-Advisor

Anthony J. Healey
Chairman, Department of Mechanical & Astronautical Engineering

THIS PAGE INTENTIONALLY LEFT BLANK

ABSTRACT

Future Navy Capabilities indicate the need for a supersonic cruise missile. Therefore, there exists a need for a low cost, light-weight, and efficient means of supersonic propulsion. NPS has been developing the Pulse Detonation Engine, which in theory has a thermodynamic efficiency greater than 50% as compared to 35% for state of the art constant-pressure cycles currently in use in gas turbines/ramjets/scramjets. Nonetheless, there are two major problems in the development of this engine. These are the increase of the propulsive efficiency by removing the oxygen-assisted initiator currently in use, and the reduction of internal total pressure losses caused by the highly constrictive internal flow-path geometry currently required to promote the deflagration to detonation transition (DDT). The aforementioned problems have been addressed and a viable design proposed through the implementation of a novel Transient Plasma Ignition system and novel split-flow path engine geometry as described in this work. Future work will concentrate on the development of a performance measurement test rig to experimentally assess the designs presented herein.

THIS PAGE INTENTIONALLY LEFT BLANK

TABLE OF CONTENTS

| | | |
|-------------|--|-----------|
| I. | INTRODUCTION..... | 1 |
| A. | THEORY | 1 |
| 1. | Detonation Wave Theory | 1 |
| 2. | Transient Plasma Ignition | 5 |
| 3. | Deflagration to Detonation Transition..... | 6 |
| B. | PREVIOUS WORK..... | 8 |
| C. | OBJECTIVES | 9 |
| II. | DISCUSSION OF COAXIAL FLOW DESIGN CONSIDERATIONS..... | 11 |
| A. | COAXIAL SPLIT FLOW DESIGN CONCEPT | 11 |
| B. | DISCUSSION OF COAXIAL INLET FLOW DESIGN..... | 15 |
| C. | DISCUSSION OF ANNULAR ELECTRODE DESIGN | 17 |
| 1. | Discussion of ceramic insulator design | 20 |
| 2. | Discussion of TPI/Electrode Interface | 23 |
| 3. | Discussion of DDT Region..... | 25 |
| III. | RESULTS | 27 |
| IV. | CONCLUSIONS AND FUTURE WORK..... | 31 |
| | APPENDIX A: COMPONENT DRAWINGS..... | 33 |
| | LIST OF REFERENCES | 41 |
| | INITIAL DISTRIBUTION LIST | 43 |

THIS PAGE INTENTIONALLY LEFT BLANK

LIST OF FIGURES

| | | |
|------------|--|----|
| Figure 1. | Stationary One-Dimensional Combustion Wave (From Ref. 3)..... | 3 |
| Figure 2. | ZND One-Dimensional Wave Structure (From Ref. 5)..... | 4 |
| Figure 3. | Three-Dimensional Detonation Wave Structure (From Ref. 5)..... | 5 |
| Figure 4. | Streamer Wave Front from a TPI Electrode (From Ref. 7) | 6 |
| Figure 5. | Deflagration to Detonation Transition Schlieren Images (From Ref. 8) | 8 |
| Figure 6. | Annular and Center Flow Paths | 11 |
| Figure 7. | Time-lapse Simulated View of Shock-to-Shock Interaction (From Ref. 9) | 13 |
| Figure 8. | Convex and Concave Flanges for Coaxial Flow Inlet | 16 |
| Figure 9. | Coaxial Inlet Flow Design | 17 |
| Figure 10. | Rod Electrode vs. Annular Electrode..... | 17 |
| Figure 11. | Cross Section View of Annular Electrode..... | 18 |
| Figure 12. | Ceramic Insulator used in previous PDE test engines (From Ref. 3) | 19 |
| Figure 13. | Failure of Existing Ceramic Insulator Threads | 20 |
| Figure 14. | Ceramic Head Flange Insulator | 21 |
| Figure 15. | Ceramic Aft Insulator | 22 |
| Figure 16. | Electrode with Insulators mounted to Head Flange..... | 23 |
| Figure 17. | TPI/Electrode Interface | 24 |
| Figure 18. | TPI/Electrode Interface Mounted to Test Engine | 24 |
| Figure 19. | DDT Region..... | 25 |
| Figure 20. | Cross Section View of Coaxial Split Flow PDE Design | 27 |
| Figure 21. | Isometric View of Coaxial Split Flow PDE (Outer Tube shown transparently) | 27 |
| Figure 22. | Section View of Coaxial Split Flow PDE showing Implosion Phenomena | 28 |
| Figure 23. | Total Internal Pressure Loss vs. Flow Rate for Existing PDE and Coaxial Split Flow Designs (From Ref. 9)..... | 29 |
| Figure 24. | Head Flange | 33 |
| Figure 25. | Inlet Flow Flange | 34 |
| Figure 26. | Inlet Flow Backing Plate..... | 35 |
| Figure 27. | Head Flange Insulator | 36 |
| Figure 28. | Aft Insulator | 37 |
| Figure 29. | Anode..... | 38 |
| Figure 30. | Initiator Tube | 39 |
| Figure 31. | Initiator Tube Connecting Flange | 40 |

THIS PAGE INTENTIONALLY LEFT BLANK

LIST OF TABLES

| | | |
|----------|---|---|
| Table 1. | Differences in Thermodynamic Conditions for Detonation and Deflagration (From Ref. 3) | 3 |
|----------|---|---|

THIS PAGE INTENTIONALLY LEFT BLANK

ACKNOWLEDGMENTS

The author would like to express his profound gratitude to Professor Jose Sinibaldi for the help, guidance, and education he so patiently provided while this thesis work was completed. This would not have been achieved without his dedicated assistance and sense of humor.

The author would also like to thank Professor Christopher Brophy for his guidance and assistance, as well as that of George Hageman and CAPT Patrick Hutcheson, CAF. This thesis would truly have never been possible without the support of our sponsors at the Office of Naval Research.

Finally, the author would like to express his gratitude to the support of his wife, Laura, in this and all endeavors.

THIS PAGE INTENTIONALLY LEFT BLANK

I. INTRODUCTION

The Navy is currently interested in developing Pulse Detonation Engines (PDE) as a low-cost, simple, light-weight, and efficient means of supersonic propulsion. The PDE concept has a higher thermodynamic efficiency than the constant-pressure cycles currently in use, such as turbojets, ramjets, and scramjets. A major problem in the development of this type of engine is increasing the propulsive efficiency to acceptable levels. Previously, achieving successful detonations in the engines tested at the Naval Postgraduate School (NPS) required an oxygen-assisted initiator unit which subsequently initiated the detonation in a fuel/air mixture. Auxiliary oxygen-enriched air added to an air-breathing engine is often treated, in effect, as a fuel and must be considered as such when computing the fuel-based specific impulse. This is shown below in Equation (1). The result is a much lower specific impulse than if the engine could run without auxiliary oxygen.

$$I_{sp_f} = \frac{F}{\dot{m}_{fuel} g} = \frac{F}{(\dot{m}_{fuel} + \dot{m}_{fuel_init} + \dot{m}_{O_2_init}) g} \quad (1)$$

The dependence on an oxygen-assisted initiator must be removed if the practical development of the PDE is to proceed. Through the implementation of the state-of-the-art Transient Plasma Ignition (TPI) technology and novel engine flow geometry, oxygen-assisted initiators will no longer be necessary. To understand how this problem might be solved, the theory of detonations and PDEs must be addressed.

A. THEORY

1. Detonation Wave Theory

The combustion process is an inherent mechanism in any propulsion system which relies on high enthalpy combustion products for thrust generation. Combustion processes can be most easily classified as either deflagrations or detonations. Deflagration is a subsonic combustion wave which propagates by means of both mass and thermal diffusion. This type of combustion is generally easier to control and used

when a system operates in a steady-state mode. Examples of deflagration applications are internal combustion engines and combustion chambers in turbojets, ramjets, among others.

In contrast to deflagration, detonation is supersonic combustion which can be thought of as a shock wave coupled with a reaction zone. As the detonation wave propagates, the shock wave compresses the reactants and causes the combustion process to occur at a much higher pressure. Detonation waves are defined by Glassman as “a shock wave that is sustained by the energy of the chemical reaction in the highly compressed explosive medium existing in the wave” [1]. This process occurs over such a short period of time that detonations can be closely approximated to a constant-volume combustion process. It is this approximation that makes PDE development so promising since it is well known that an engine based on a constant-volume combustion process will have a higher thermodynamic efficiency than an engine based on a constant-pressure process.

The theory behind the physical nature of detonation waves was first developed over a century ago. Chapman (1899) and Jouguet (1905-6) presented theories of detonation waves after successfully carrying out detonations in an experimental setting. Chapman and Jouguet (CJ) obtained two significant results by examining continuity of mass, energy, and momentum in the axial direction. The first result was the steady-state value of detonation wave velocity, known as *CJ-velocity* in their honor. The second result was to obtain thermodynamic conditions of combustion products immediately behind the detonation wave. These conditions, particular to detonation wave propagation, are known as *CJ conditions* [2]. Figure 1 shows a stationary one-dimensional combustion wave and Table 1 describes the differences between the thermodynamic conditions across a deflagration and detonation combustion wave.

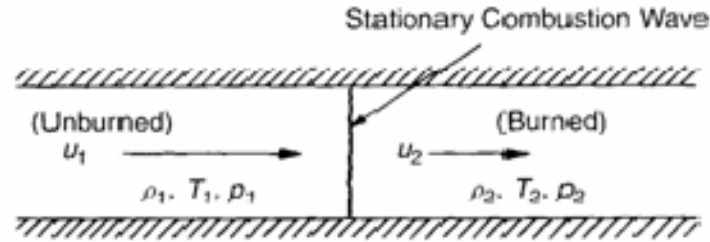


Figure 1. Stationary One-Dimensional Combustion Wave (From Ref. 3)

| | Detonation | Deflagration |
|-----------------|------------------------|-------------------------------|
| u_1/c_1 | 5-10 | 0.0001-0.03 |
| u_2/u_1 | 0.4-0.7 (deceleration) | 4-16 |
| p_2/p_1 | 13-55 (compression) | 0.98-0.976 (slight expansion) |
| T_2/T_1 | 8-21 (heat addition) | 4-16 (heat addition) |
| ρ_2/ρ_1 | 1.4-2.6 | 0.06-0.25 |

Table 1. Differences in Thermodynamic Conditions for Detonation and Deflagration (From Ref. 3)

Improving upon the detonation wave theory nearly forty years after the first experiments were performed, Zeldovich, von Neumann and Doring (ZND) considered chemical induction time in similar detonation wave models used by Chapman and Jouguet [4]. Since the work of ZND was an extension of the work performed by CJ, the models yielded nearly identical detonation wave velocities and thermodynamic conditions of the products. The introduction of chemical induction time did, however, allow for the ZND model to calculate a finite detonation wave thickness while the CJ model assumed it to be infinitesimal.

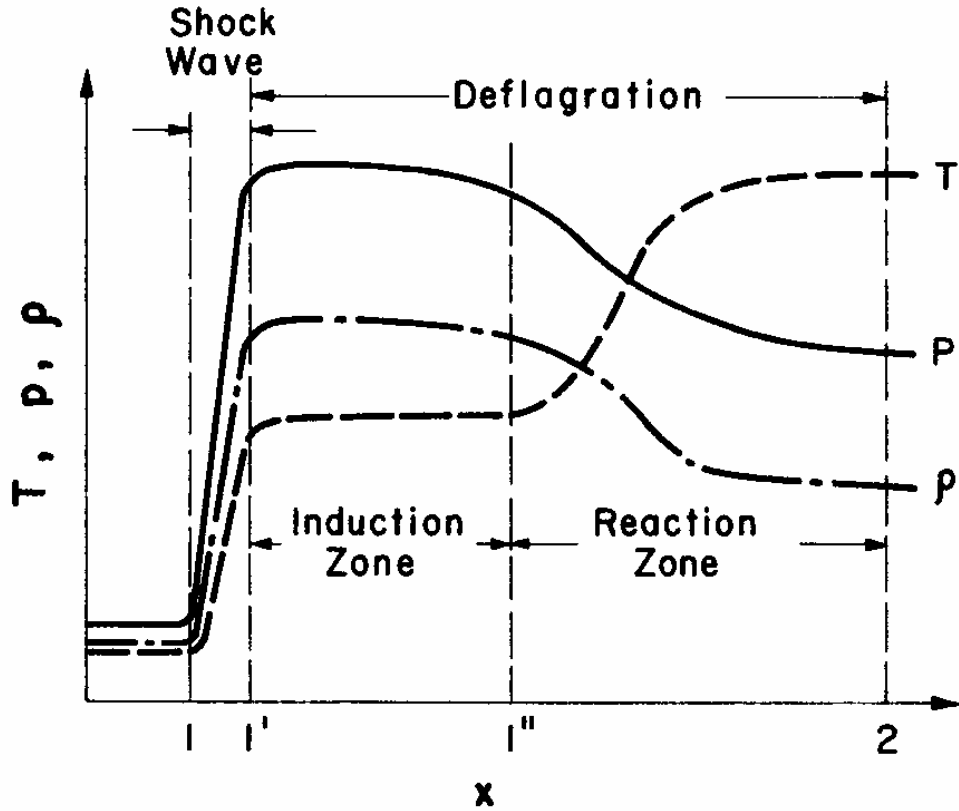


Figure 2. ZND One-Dimensional Wave Structure (From Ref. 5)

The ZND one-dimensional detonation wave structure in Figure 2 shows that pressure, density, and temperature rise sharply as the planar shock wave travels through the reactants. The thermodynamic properties maintain their values relative to one another through the induction zone, and then the properties change abruptly as energy is released in the reaction zone.

While the ZND model accurately describes the process in one dimension, actual detonation wave structure is far more complex than can be accounted for in one-dimensional modeling. Understanding of detonation wave structure is critical to wave behavior analysis and PDE design. Further discussion of multi-dimension wave structure analysis can be found in reference [6]. Figure 3 provides an example of the three-dimensional structure of detonation waves, as well as the cell size, λ .

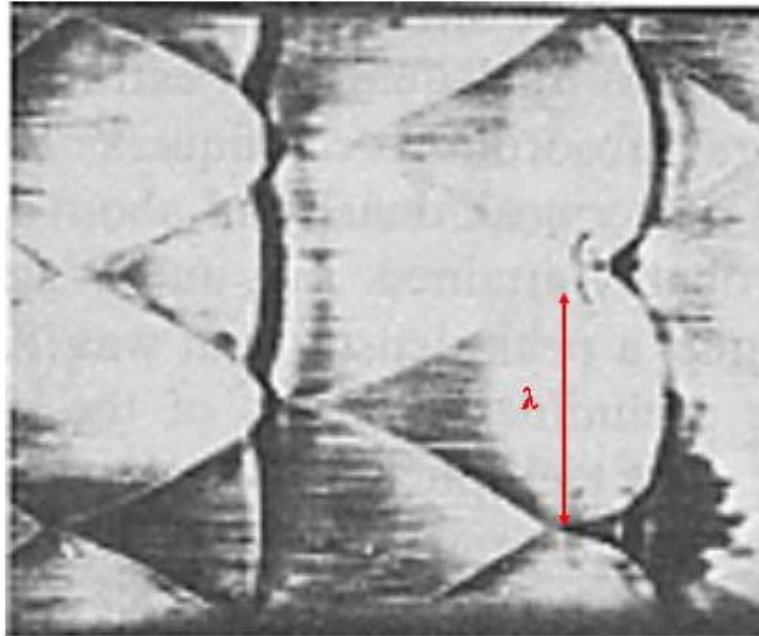


Figure 3. Three-Dimensional Detonation Wave Structure (From Ref. 5)

The cell size, λ , is a characteristic length which is indicative of the sensitivity of a mixture and is inversely related to the size of the induction zone. Highly sensitive mixtures generally have a smaller cell sizes and are more easily detonable. Empirical work has also shown that there exists a critical tube diameter, d_c , which will allow a detonation wave to continue as a spherical wave when it transitions from the end of the tube to an unconfined space containing the same mixture. This critical diameter was found to be thirteen times the cell size, $d_c = 13\lambda$ [1].

2. Transient Plasma Ignition

Transient plasma discharge is the transient phase of an electrical discharge before arc formation. Experiments at the University of Southern California have shown that the energy in the transient plasma discharge is much more efficient for flame ignition than the energy in arc and glow discharges. In conventional spark discharge, only a small percentage of the energy goes to the transient phase while the bulk of the energy goes to arc and glow discharges. Transient Plasma Ignition (TPI) technology discharges higher

voltages (at least 50 kV) than conventional spark discharges and creates a streamer wave front. An example of a typical streamer wave front from a rod electrode is shown in Figure 4.

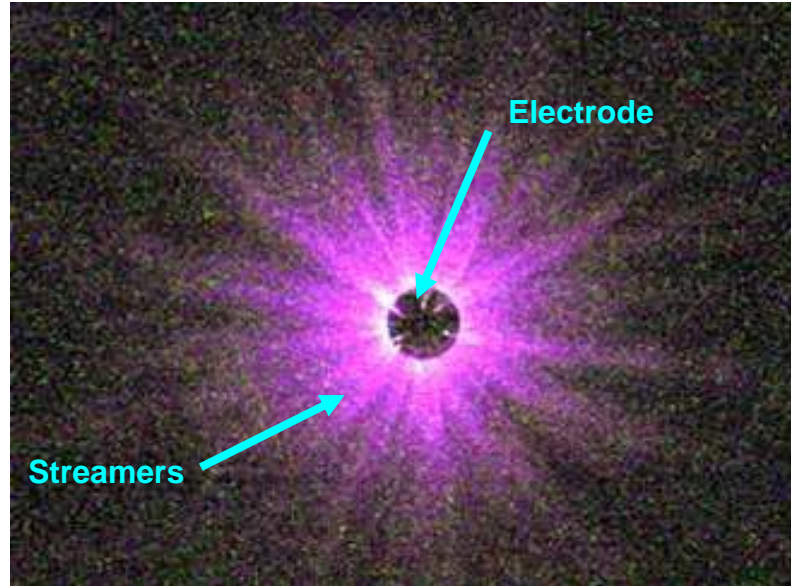


Figure 4. Streamer Wave Front from a TPI Electrode (From Ref. 7)

Within the high electric field of these streamer wave fronts can exist energetic electrons (on the order of 10 to 20 eV compared to 1 eV for conventional spark discharge) with high kinetic energies that can effectively generate reactive species such as O atom, H atom, the flame front marker CH, which very quickly react to produce the chain branching radical OH, which can rapidly initiate chain reactions. Due to the rapid generation of these reactive species, transient plasma discharges can readily ignite a flame at many points simultaneously, as opposed to only one discharge channel in conventional spark ignition [7]. Because flame ignition occurs over many points rather than only one, the transition from laminar to turbulent flame occurs much faster in a transient plasma discharge than in conventional spark discharge.

3. Deflagration to Detonation Transition

Deflagration to Detonation Transition (DDT) is the process by which a laminar flame changes propagation mechanisms and eventually develops into a self-sustaining detonation wave. For optimal DDT performance, both time and distance over which the

transition occurs, is to be minimized. DDT can be summarized in five steps: (1) Ignition and wave propagation. (2) Flame wrinkling, turbulence onset, and dramatic increase in burning rate. (3) Increased burning rates increase flow velocity ahead of the mixture due to expanding gases. Unsteady compression waves ahead of the flame front increase temperature sufficiently to produce an acceleration effect on reaction rates. Shock front formation occurs due to the coalescence of compression waves. (4) Detonation onset, “explosion in an explosion”, in which there is an abrupt appearance of explosion centers or “hot spots” in the shock. (5) The detonation wave propagates, if successfully formed, developing into a pseudo-steady, self-sustaining wave at a CJ wave speed and thermodynamic conditions [8]. Figure 5 shows, through a series of stroboscopic Schlieren images, DDT from the work done by Urtiew and Oppenheim.

DDT can be aided by inserting obstacles in the flow path and through the use of TPI. The intentional obstacles placed into the flow path create blockages which lead to local increases in turbulence, temperature, and pressure, which encourage DDT as the flow negotiates the obstacles. TPI accelerates the DDT process by increasing the number of flame ignition sites within the reactants and decreasing the laminar-to-turbulent transition time. Because the laminar-to-turbulent flame transition comprises the majority of the time required for DDT, decreasing the transition time to achieve a turbulent flame is critical to minimizing DDT time.

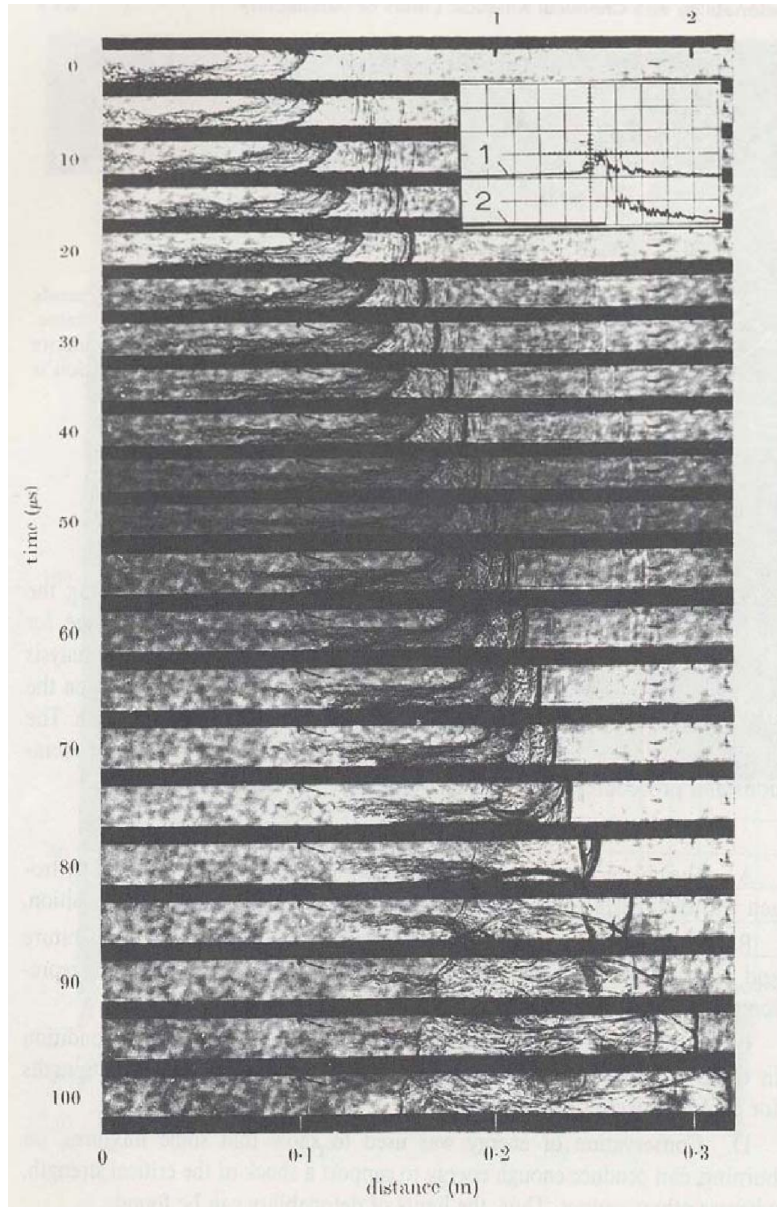


Figure 5. Deflagration to Detonation Transition Schlieren Images (From Ref. 8)

B. PREVIOUS WORK

Previous work at the NPS Rocket Propulsion Laboratory (RPL) which has given insight into potential areas of improvement of PDE performance has been conducted by Rodriguez [5] and Channell [3] in their Master's Theses in 2005. Rodriguez studied Transient Plasma Ignition (TPI) strategies and concluded that TPI technology was a more effective and reliable ignition system compared to high-performance Capacitive Discharge spark plug ignition systems. TPI technology decreased the DDT distance by

nearly 10% and DDT time by nearly 33%. Rodriguez also concluded that due to these improvements, most of if not all of the oxygen-assisted initiator requirements could be removed.

Channell studied fuel/air initiation strategies and concluded that TPI could provide consistent ignition at higher flow rates (> 0.10 kg/s), which high-performance capacitive discharge systems could not. He also observed that TPI technology allowed for operating frequencies in excess of 40 Hz and that these operating frequencies were limited not by TPI capabilities but by the increasing flow velocity through the initiator as mass flow rates were increased. He concluded that high operating frequencies could be achieved if the flow geometry were such that it could allow for high mass flow rates while at the same time reducing the velocity of the flow through the initiator. Channell successfully developed detonations up to ~ 40 Hz.

C. OBJECTIVES

There are four main objectives of this thesis. First, eliminate the need for an oxygen-assisted initiator through the integration of TPI technology. Both Channel and Rodriguez concluded that this is necessary advancement for a practical PDE. Second, decrease the overall drag of the mass flow through the engine by developing a new geometry. A practical PDE must operate at frequencies high enough to generate thrust and reducing the overall drag will allow to maintain high efficiencies at higher operating frequencies. Third, ensure the transition of detonation waves into the main core of the engine. This transition, or diffraction, should occur with minimal weakening of the detonation wave. Fourth, develop and build a design that incorporates the previous three objectives.

THIS PAGE INTENTIONALLY LEFT BLANK

II. DISCUSSION OF COAXIAL FLOW DESIGN CONSIDERATIONS

A. COAXIAL SPLIT FLOW DESIGN CONCEPT

The previous PDE geometry evaluated at NPS consisted of an inner initiator core in which the detonation developed then propagated into the larger main tube of the engine. As the detonation moved from the smaller initiator to the larger main tube, the detonation diffracted to account for the sudden difference in cross-sectional flow area. This detonation diffraction had a weakening effect on the detonation, sometimes leading to a failure to initiate a detonation in the larger main tube.

The coaxial split flow design consists of two separate flow paths which collide into one another in the main engine tube prior to exiting the engine. The point at which this collision occurs is known as the *diffraction zone*. These two flow paths are shown below in Figure 6.

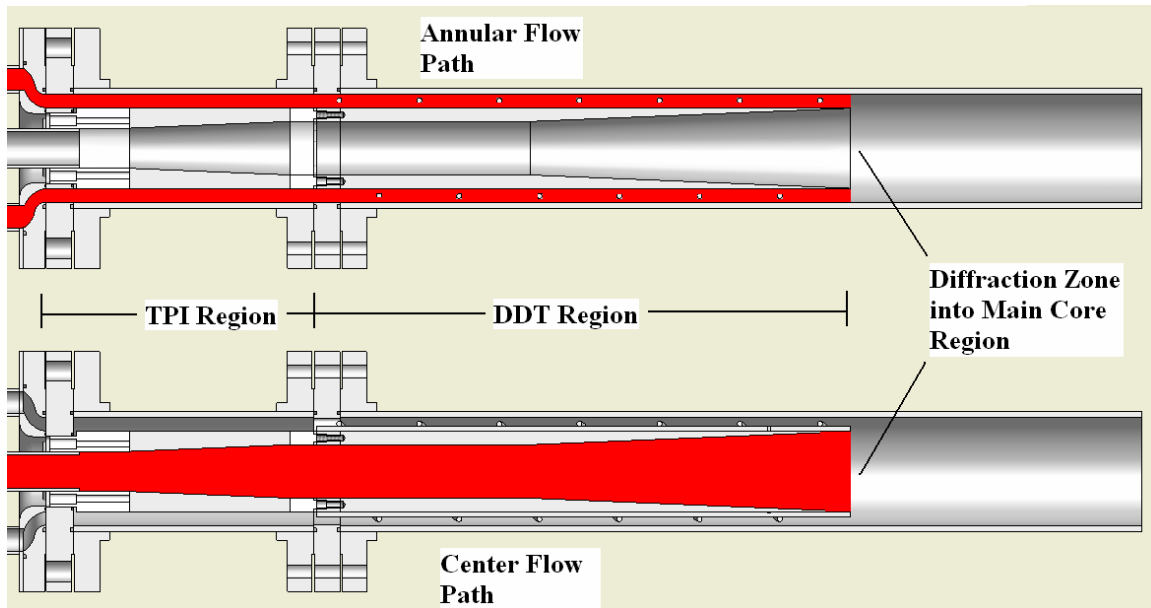
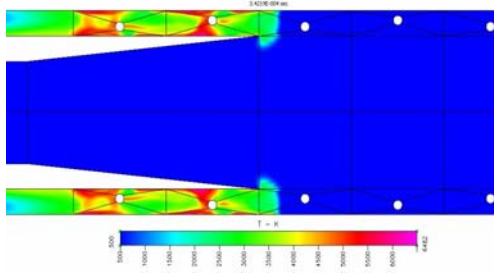


Figure 6. Annular and Center Flow Paths

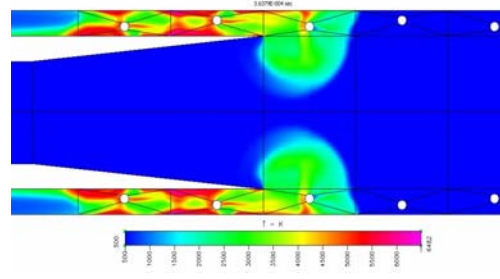
One flow path is along the centerline of the engine through a smooth, straight pipe. This flow path is known as the *center flow path*. The purpose of this flow path is to create a fast moving flow with minimal drag. The second flow path runs coaxially with the first flow path and it is in this region that this initiation takes place. This flow path is

known as the *annular flow path*. The purpose of this region is to slow the flow to allow for adequate flame development. Since an annular region has two surfaces on which the flow interacts, the drag in this region is substantially higher than in the first flow path. Furthermore, the spirals which assist detonation development are confined to this region, which also increases the drag. Increasing drag, however, in the region where detonation development is to occur is not necessarily undesirable since drag introduces turbulence, which greatly promotes DDT.

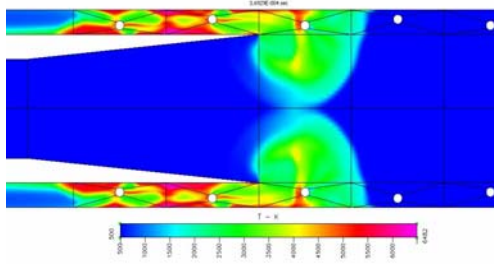
Similar to previous PDE designs, the detonation must diffract as the initiator merges into the main tube of the engine. The difference is that in the coaxial split flow design, the detonation diffracts towards the centerline and not from the centerline. When the detonation converges on the centerline of the engine, the shock-to-shock interaction that takes place should result in high temperatures and pressures and ignite the fast moving reactants flowing directly into the detonation convergence. As has been shown by Shepherd's research group at Caltech, imploding detonation waves can produce enormous pressures and temperatures [9]. Figure 7 presents a time-lapse simulated view of the shock-to-shock/implosion phenomena taking place.



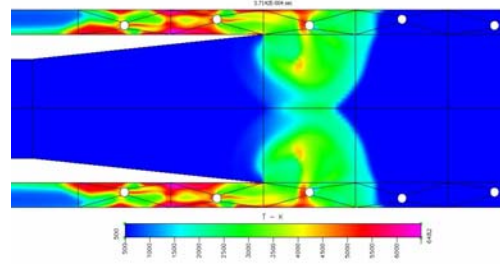
7.1



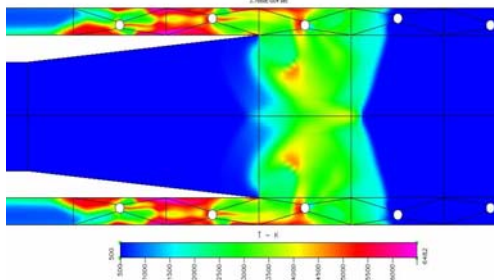
7.2



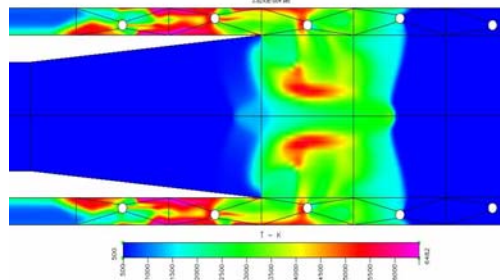
7.3



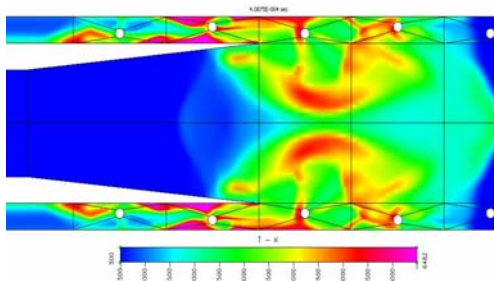
7.4



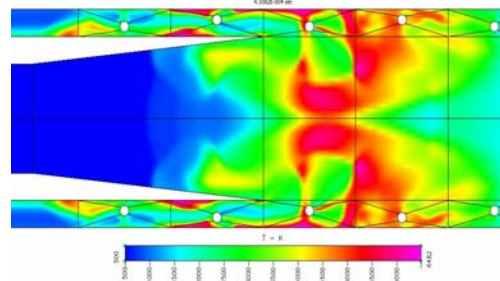
7.5



7.6



7.7



7.8

Figure 7. Time-lapse Simulated View of Shock-to-Shock Interaction (From Ref. 9)

The eight images in Figure 7 are cross-section views of the diffraction zone. Holthaus ran these simulations using CFD-FASTRAN [10]. For this particular case, Holthaus has assumed an annular Mach number of 5 and a Mach number of zero in the center region. The color scale represents a temperature gradient, ranging from ~500 K (blue) to ~6000 K (red) [10]. Further explanation for the temperature gradients observed in the images in Figure 7 can be found in Holthaus thesis, Ref. 10.

From Figure 7.1, it can be assumed that DDT occurs slightly before the end of the initiator, where a drastic increase in temperature is observed. Images 7.2 to 7.4 show the detonation diffracting from the initiator into the main engine core. Images 7.5 to 7.7 show the wave implosion phenomena as it diffracts from the annular initiator. Image 7.8 is of particular importance because it shows large zones of extremely high temperatures (red and purple zones) in the center flow path. This supports the hypothesis that the shock-to-shock interaction/implosion phenomena will generate high temperatures to directly initiate a detonation wave in the fuel-air mixture passing through the center flow path. This is of particular significance because at present, existing multi-cycle PDEs have experienced a weakening of detonation wave as the wave diffracts from the initiator into the main core. The design presented here, modeled by Holthaus, suggests the opposite. As the detonation wave diffracts in the coaxial split flow PDE, the shock-to-shock interaction is enhanced and has the potential to strengthen the detonation wave as it diffracts.

There are two separate sections of the engine, which allow it to be broken down and parts to be interchanged depending on the desired test scenarios. The first section, situated between the two sets of flanges, contains the electrode. The second section, from the second set of flanges to the end of the engine, serves two primary purposes. First, the tube in the center of this section extends the length of the initiator region to approximately thirty inches. It has been empirically shown that this is the optimal length for detonation wave formation. Second, detonation diffraction occurs in this region. At the end of the initiator region, the shock remaining from the detonation wave begins to implode not only into itself, but also into the fast-moving reactants traveling through the center flow path. As previously stated, it is at this point that the shock-to-shock interaction should take place.

The center flow path of the electrode was tapered to create a diverging nozzle. The reason for tapering the electrode was to smoothly decelerate the center flow as soon as possible after passing through the highly space restrictive head-flange in order to further lower the pressure losses which in a smooth tube are directly relate to the fill mach number. Therefore, the flow is expanded through the electrode from an inlet area of 1.767 in² (1.5 in diameter) to 3.14 in² (2 in diameter). The divergence angle through the electrode is 4.76° to prevent flow separation, which generally occurs when the flow is diverged at angles greater than 14°.

B. DISCUSSION OF COAXIAL INLET FLOW DESIGN

Delivering mass flow to two separate, coaxial flow paths was a new problem in PDE design. Approximately 50% of the mass flow was to be sent through a smooth path, which yielded a lower total pressure loss. The remainder of the mass flow was to be sent through an annular initiator, which may include obstacles to aid the DDT process. The innovative design employs a center path (flow in a smooth pipe has the minimal pressure losses) and a second region flowing coaxially in which a Schelkhin spiral is mounted to promote DDT. Delivering mass flow to the center flow path could be easily accomplished. Delivering mass flow to the annular flow path was inherently more difficult, not only because of the geometry, but also because the inlet design had to allow accessibility to the ceramic head flange insulator for the TPI interface. By machining a concave hole into one blind flange, and a convex hole into another, the desired affect was achieved. These two flanges and a section view of the flanges assembled are show in Figure 8.

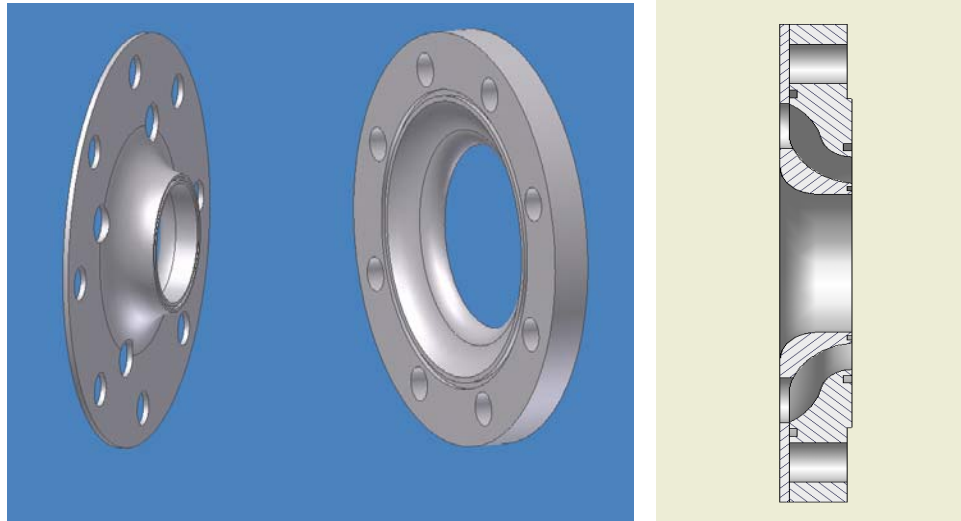


Figure 8. Convex and Concave Flanges for Coaxial Flow Inlet

Air is heated through the use of a vitiator which raises the temperature of the reactants to simulate supersonic stagnation conditions prior to the fuel injection section designed by Robbins [11]. In order to allow for proper mixing and evaporation of fuel droplets to occur, the flow was split approximately 5 diameters downstream of the fuel injection location. Fifty percent of the flow was sent through a center tube and the rest split through 4 arm tubes. The four holes surrounding the center hole of the convex flange are where the mass flow from the four arms enters the annular flow path. The flow coming from the vitiator was passed through $\frac{3}{4}$ in pipes in which chokes can be placed to adjust for desired mass flow rates. The flow delivered to the center flow path was delivered through a tube with an inner diameter of 1.25 in, in which chokes can also be placed for adjusting mass flow rates. A partially exploded view of the entire inlet design is shown in Figure 9. The red arrows in Figure 9 depict the flow paths.

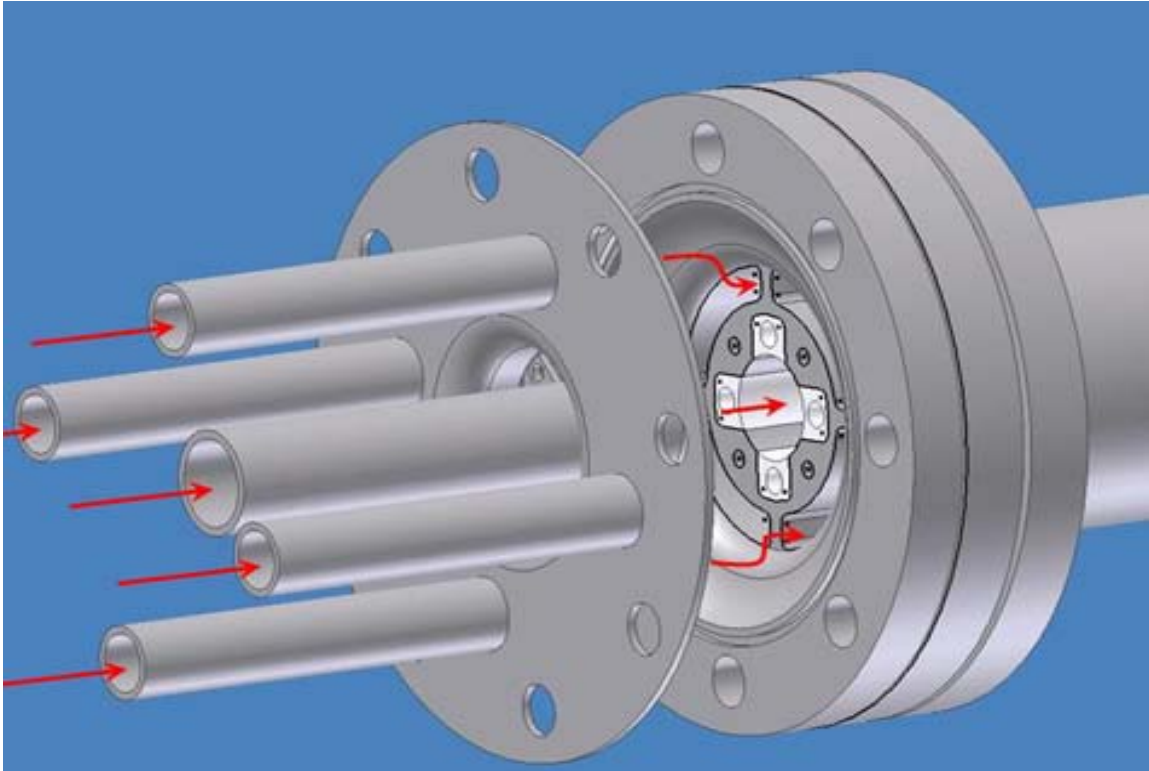


Figure 9. Coaxial Inlet Flow Design

C. DISCUSSION OF ANNULAR ELECTRODE DESIGN

While previous generations of PDEs employed a simple rod electrode, the coaxial flow design of the PDE demanded that the electrode also takes on an annular shape. Figure 10 shows a side-by-side comparison of the existing rod electrode and the electrode designed for the coaxial split flow PDE.

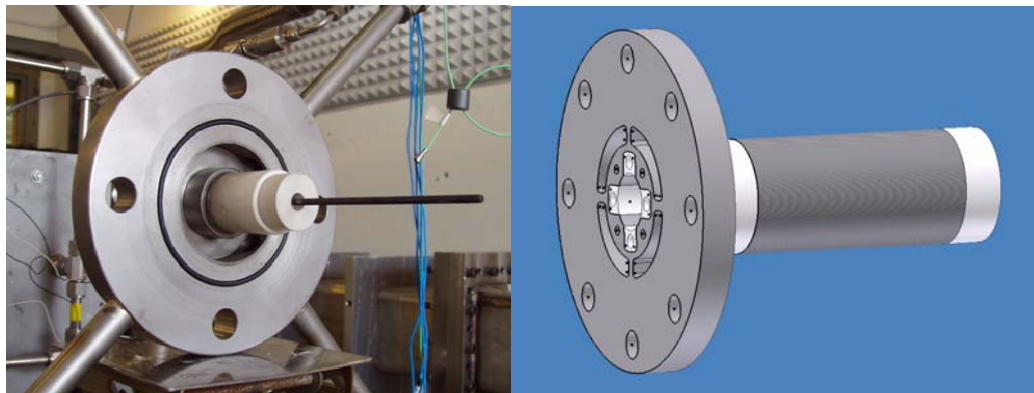


Figure 10. Rod Electrode vs. Annular Electrode

The annular electrode, like the rod electrode, requires threads over the length of the electrode where discharge will occur. Threads are machined into the electrode to promote a smooth and reliable discharge. The electrode was designed with twenty threads per inch.

The annular electrode is not merely an electrical component in this engine, but a flow channel as well. The flow is expanded through the electrode from a cross-sectional area of 1140 mm^2 to 2027 mm^2 to allow for use of more low-cost and readily available materials. The half angle of divergence is $\sim 5^\circ$ to reduce the probability of separation as the flow is expanded. In Figure 11, the TPI region of the engine is shown. The electrode is shown in yellow and the flow through the center of the engine is shown in red.

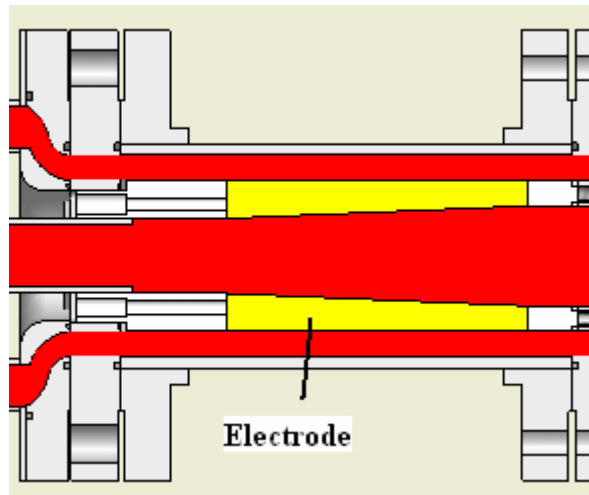


Figure 11. Cross Section View of Annular Electrode

Increasing the complexity of electrode geometry from a rod to an annular shape introduced several design challenges, predominately electrical insulation of the electrode from the rest of the engine components. From the work done by Channel, it was determined that ceramics would be most capable of withstanding the heat and pressure of detonations while providing sufficient electrical insulation for high voltages involved with transient plasma ignition [3]. The ceramic selected was Macor®, a machinable glass ceramic manufactured by Corning. This particular ceramic was selected because it withstands high temperatures ($>1000^\circ\text{C}$), has a thermal expansion coefficient, α , similar to steel ($\alpha_{\text{Macor}} = 126 \times 10^{-7}/^\circ\text{C}$ compared to $\alpha_{\text{stainless}} = 178 \times 10^{-7}/^\circ\text{C}$ for 304 Stainless Steel), will not deform at high temperatures, and has excellent dielectric strength (40 kV/mm).

Currently, TPI systems discharge approximately 80 kV, therefore, the minimum insulation thickness at any point along the path must be 2 mm. The minimum design insulation thickness was 2.5 mm to provide insulation up to 100 kV.

Previous PDE designs insulated the electrode by using a simple ceramic cylinder threaded into the head flange of the engine through which passed the rod electrode. This feature could not be utilized in the coaxial design due to the flow desired through the center of the head flange. Shown below in Figure 12 is an example of the style of ceramic insulators used in previous PDE designs.

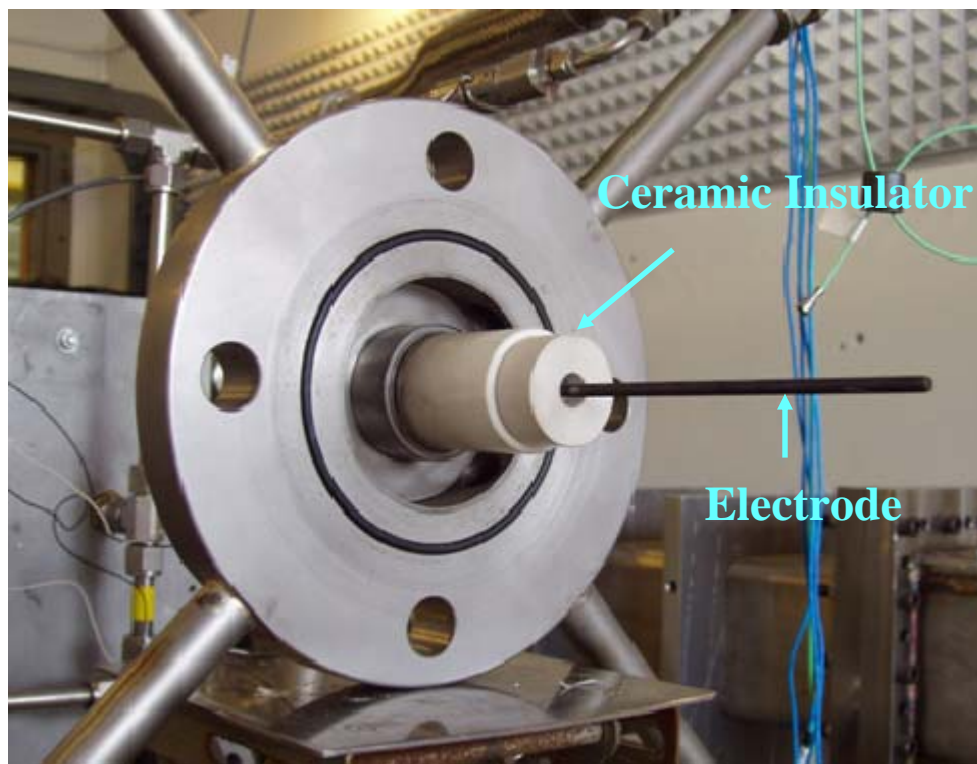


Figure 12. Ceramic Insulator used in previous PDE test engines (From Ref. 3)

The annular electrode must be insulated such that it can freely discharge radially to the inner wall of the outermost tube while avoiding a discharge to the head flange of the engine or the rest of the initiator. The leads connecting the electrode to the high voltage source needed to be insulated as well.

1. Discussion of Ceramic Insulator Design

While ceramic insulators in previous PDE designs were machined into much simpler geometries, they did not take advantage of the physical properties inherent to ceramics. Under the same conditions, ceramics will generally perform better in compressive loading than in tensile loading. Past ceramic insulators used screw threads to mount the insulator to the head flange and also to secure the electrode to the end of the insulator. Figure 13 shows an example of existing ceramic insulator threads that have failed.



Figure 13. Failure of Existing Ceramic Insulator Threads

The tensile loads under which both sets of threads were subjected led to brittle failure in these insulators. Further observation of the failed insulators revealed that the threads also introduced severe stress concentrations which also attributed to failure. For these reasons, it was decided that screw threads should be left out of any future ceramic designs and, if possible, any loading applied to ceramic members would be in compression. The part designed to insulate the electrode and electrical leads from the head flange is shown below in Figure 14.

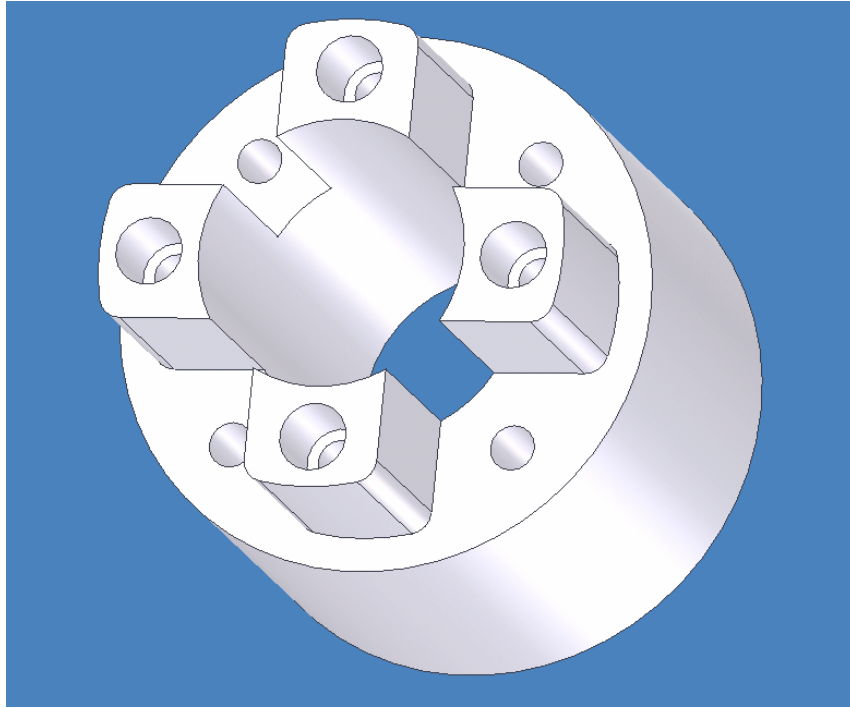


Figure 14. Ceramic Head Flange Insulator

There are four countersunk holes drilled on both the flat and the extended surfaces. The holes on the flat face are for mounting the ceramic to the head flange. Once the ceramic is mounted, the remaining space within the countersunk portion of the hole will be filled with silicone insulation to isolate the mounting bolts from the electrode. The holes drilled through the extended surfaces will insulate the electrical leads connecting the electrode to the TPI equipment. By mounting the ceramic insulator in this way, the possibility of brittle failure will be reduced as the member will be firmly compressed between the head flange and the electrode. The distance from the electrode to the wall to which it will discharge is 0.5 inch. To avoid undesirable discharge, surfaces to which discharging is not intended should be greater than one and a half times the desired discharge distance. The insulator extends the electrode one inch (two times the desired discharge distance) from the surface of the head flange to reduce the possibility of undesirable discharges.

The part which insulates the aft end of the electrode is shown in Figure 15. This part was designed with the same concepts in mind as the head flange insulator. This

insulator will be mounted to the aft end of the electrode. The thickness of this insulator is one inch (two times the desired discharge distance).

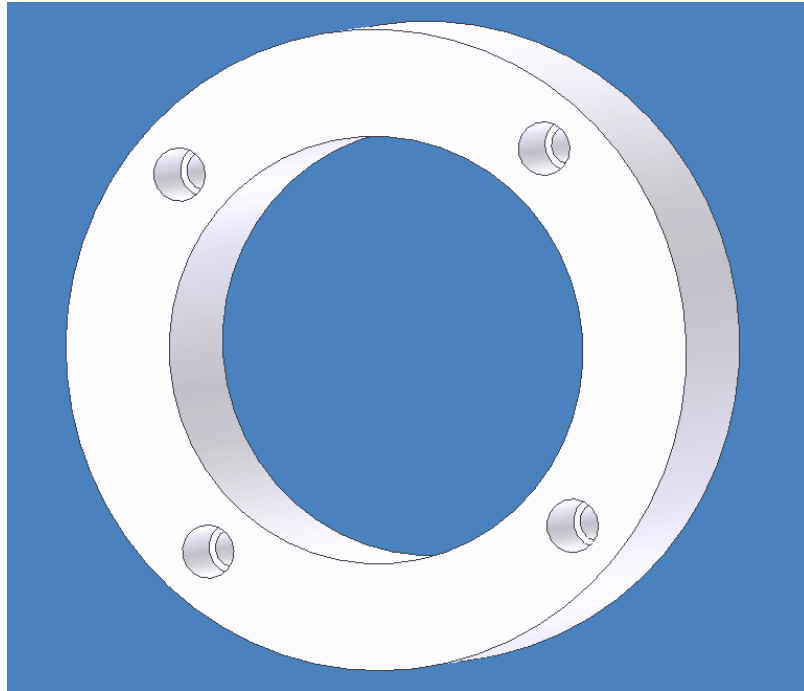


Figure 15. Ceramic Aft Insulator

Again, the remaining space within the countersunk holes will be filled with silicone insulation to isolate the electrode from the rest of the engine. This insulator will be firmly compressed between the electrode and the aft tube which separates the main flow from the initiator. Figure 16 shows an assembly of the electrode with both insulators mounted to the head flange.

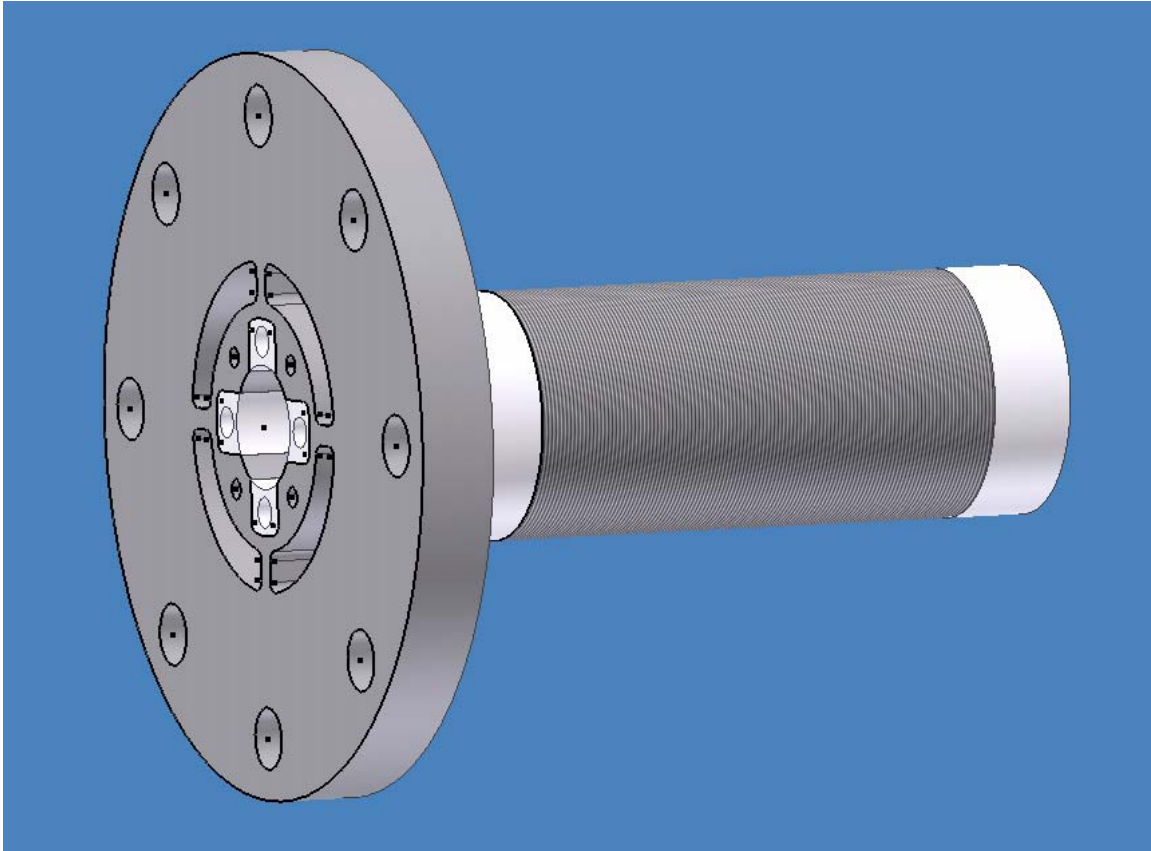


Figure 16. Electrode with Insulators mounted to Head Flange

2. Discussion of TPI/Electrode Interface

Successfully delivering a consistent and reliable high voltage charge to the electrode is essential for proper PDE performance. Interfacing TPI equipment and the electrode in previous PDE designs was as simple as plugging a banana clip into the female end of a UHF receptacle at the end of the ceramic insulator holding the electrode. With an annular electrode, the interface becomes more complicated.

The primary consideration taken in the design of this interface was to bring the electrode up to potential symmetrically. No matter how minuscule it may be, there still exists a finite amount of time for the voltage to pass through the electrode. If the TPI equipment were interfaced with the electrode through a single lead, then one side of the electrode may discharge before another side is even fully raised to potential. This could result in an unsymmetrical flame ignition within the initiator, leading to poor, or non-

existent, detonation wave formation. It was therefore decided to split the current from the TPI between two leads to the electrode. Figure 17 shows how this may be accomplished.

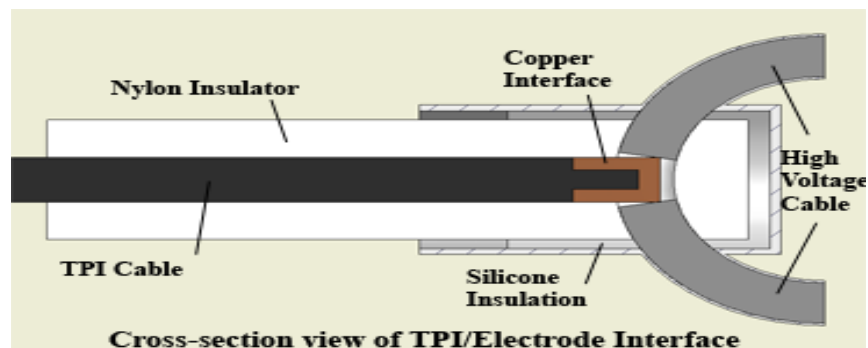


Figure 17. TPI/Electrode Interface

Two leads, 180 degrees apart, pass through the ceramic insulator. These leads were connected using high-voltage rated cable. The cable was spliced together and connected to a copper interface, to which the TPI equipment can be connected using a banana plug. The cable was shielded in thin metal to prevent any signal interference due to the high-voltage. Figure 18 shows how the TPI/Electrode Interface will be mounted onto the test engine.

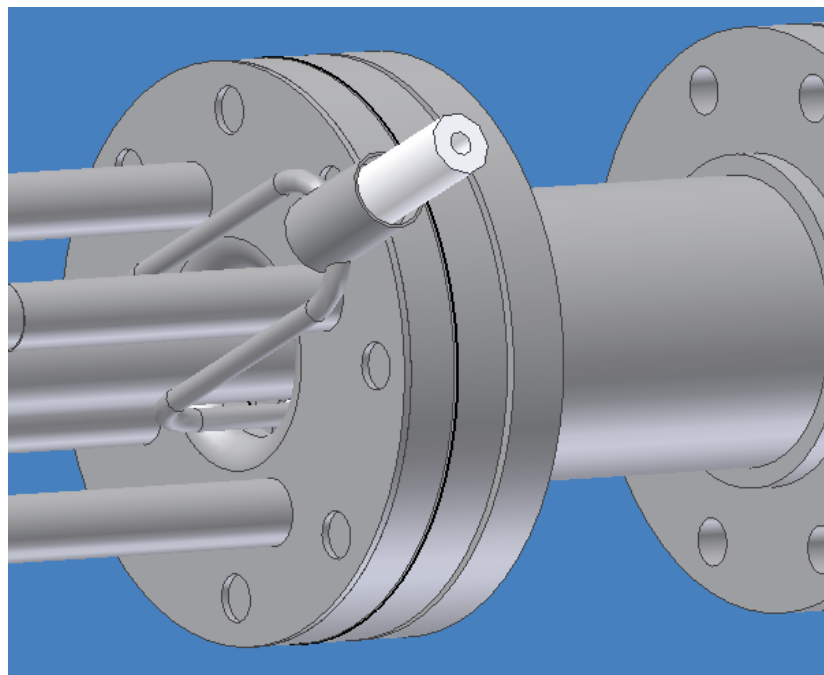


Figure 18. TPI/Electrode Interface Mounted to Test Engine

3. Discussion of DDT Region

The DDT Region of the engine consists primarily of a steel tube with a 3 inch OD and a 2 in ID which extends twenty inches past the second set of flanges. The inside of the tube is smooth and diverges at an angle of 2.39° to promote smooth flow transition, thus reducing the possibility of flow separation. Mounted on the outside of the tube is a Schelkhin spiral which serves as an obstruction to aid the DDT process. Figure 19 shows two views of the DDT region.

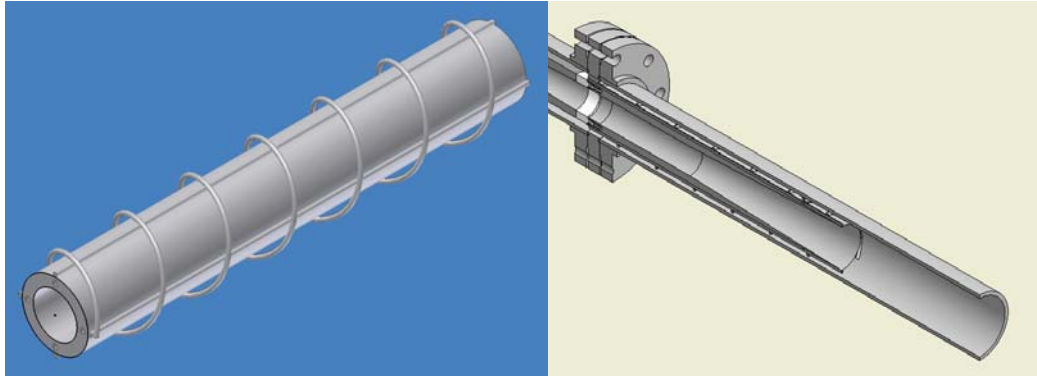


Figure 19. DDT Region

The length of this tube, and the entire engine for that matter, was determined based on previous experiments with PDEs. It has been shown that in order to achieve useful thrust levels, high frequency PDE operation (>40 Hz) is required in an outer tube diameter of at least 3. The problem is that DDT distance increases with increasing tube diameter. The engine used by Channell had a three inch ID tube and the DDT distance observed during his testing was approximately 30 inches [3]. Likewise, PDE testing performed at the Air Force Research Laboratory showed that DDT distance for a one inch ID tube was approximately twelve inches [12]. It was therefore decided that the overall length of the engine should be approximately forty inches to allow for DDT to occur. DDT in the coaxial flow engine is, however, expected to occur over shorter distances than it has in past engine designs.

THIS PAGE INTENTIONALLY LEFT BLANK

III. RESULTS

The completed design of the coaxial split flow PDE is shown in a cross section view below in Figures 20 and 21.

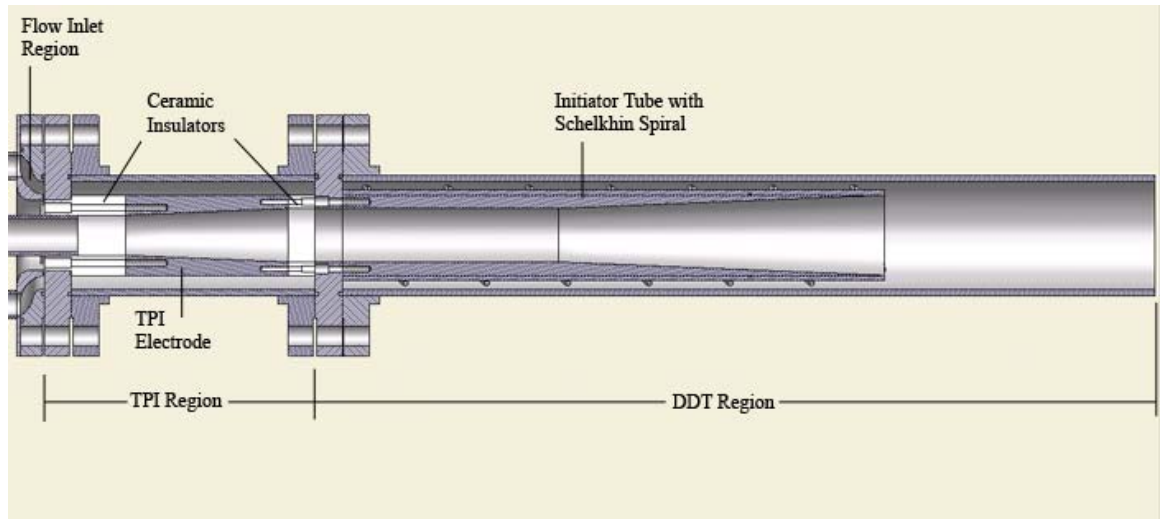


Figure 20. Cross Section View of Coaxial Split Flow PDE Design

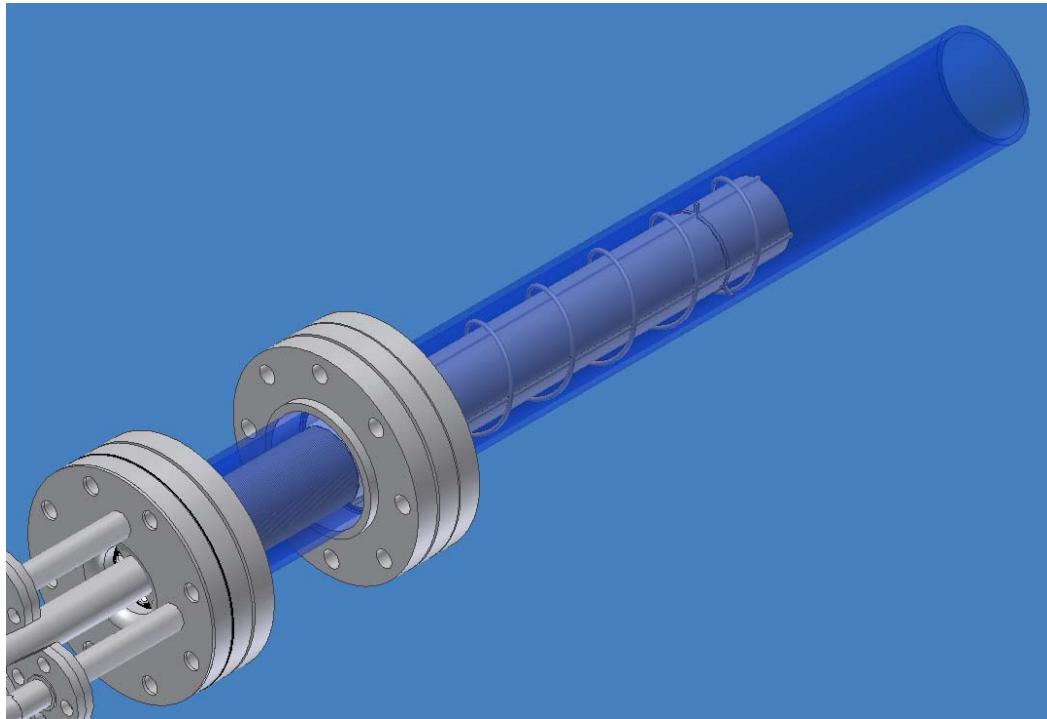


Figure 21. Isometric View of Coaxial Split Flow PDE (Outer Tube shown transparently)

Figure 22 shows simulated engine operation with temperature gradients to show where and how the shock-to-shock interaction takes place.

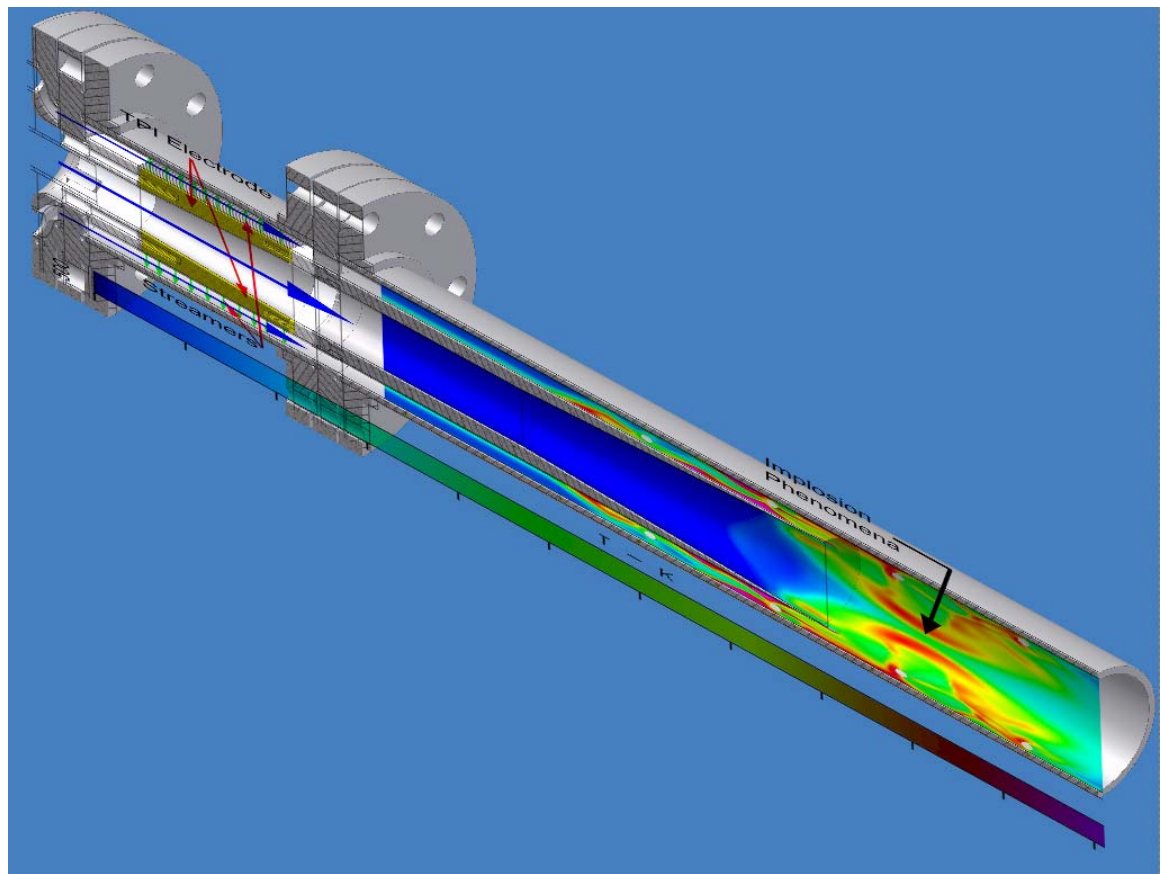


Figure 22. Section View of Coaxial Split Flow PDE showing Implosion Phenomena

The engine is currently being constructed. The timeline for completion of construction is summer of 2006, and testing is expected to follow immediately thereafter. Holthaus has shown through CFD analysis that future is promising for successful operation of this engine. Figure 23 shows a plot comparing CFD total internal pressure loss vs. flow rate of existing PDE geometry configurations compared to the coaxial split flow design with varying flow split percentages.

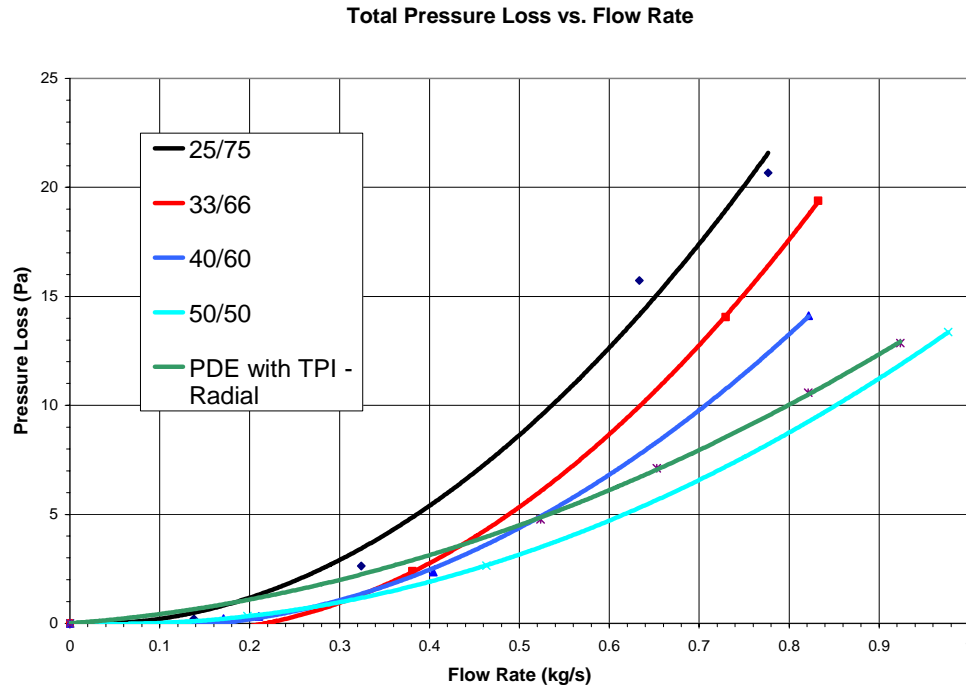


Figure 23. Total Internal Pressure Loss vs. Flow Rate for Existing PDE and Coaxial Split Flow Designs (From Ref. 9)

An objective for this design was to reduce the total internal pressure loss of the engine. The plot shows that by splitting the flow 50/50 with 50% of the flow through the center of the engine and 50% through the annular region, the total internal pressure loss will be lower than existing PDEs by nearly 1 to 2 psi for flow rates greater than 0.2 kg/s. This result is even more promising considering the fact that detonations were never actually achieved with the existing PDEs for flow rates greater than 0.4 kg/s. The coaxial split flow engine geometry should allow for mass flow rates over twice that value.

THIS PAGE INTENTIONALLY LEFT BLANK

IV. CONCLUSIONS AND FUTURE WORK

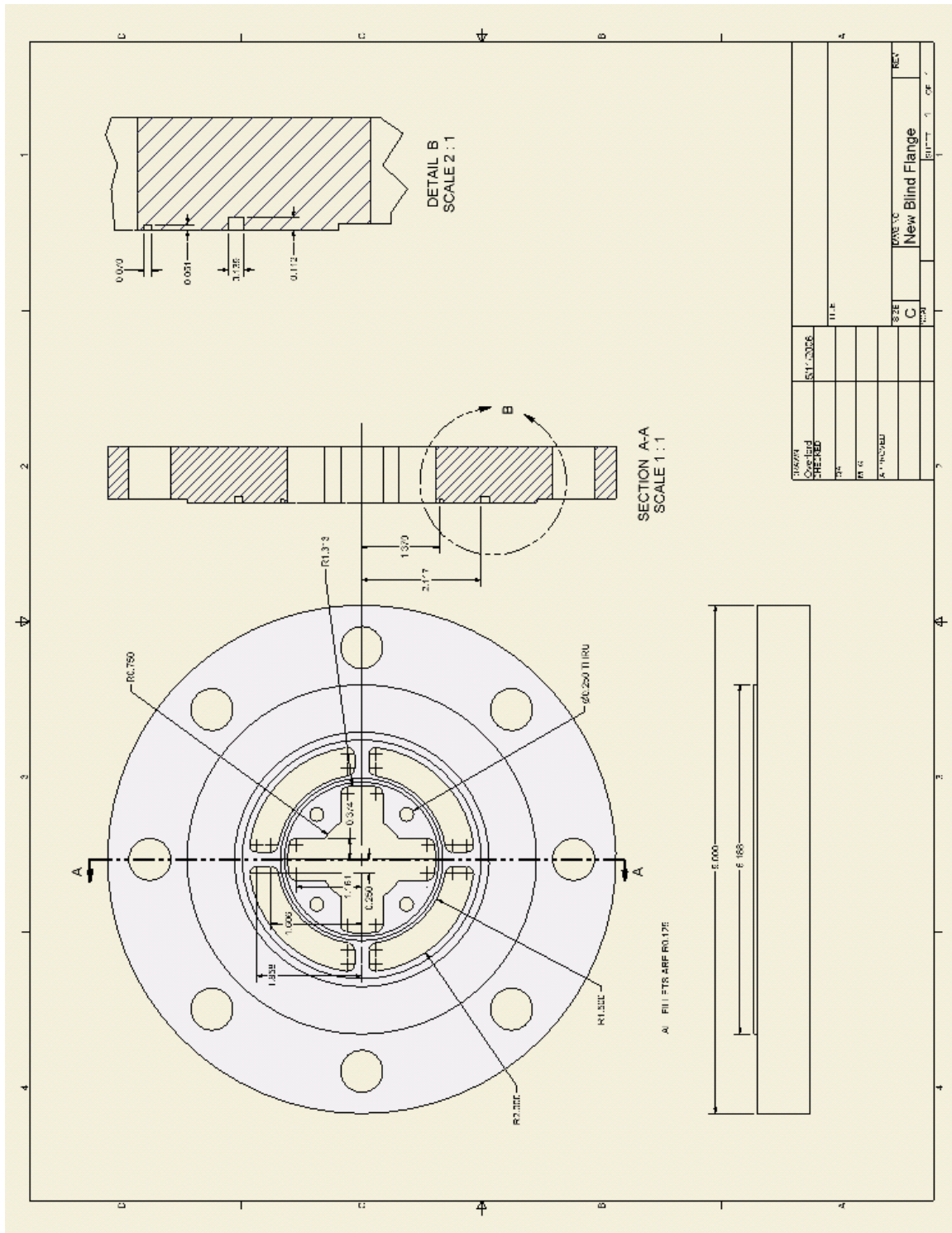
The complex geometry and component integration were achieved for a coaxial split flow PDE. An annular electrode was successfully designed which allows for both coaxial flow and TPI integration. Advanced ceramics were successfully integrated for insulating the annular electrode. The ceramic was utilized using solely compression loading, taking advantage of the physical properties inherent in ceramics.

CFD analysis performed by Holthaus has supported the concepts upon which the engine was designed. The center flow region is capable of reducing the total internal pressure loss of the engine. The shock-to-shock interaction / implosion phenomena at the diffraction region should generate temperatures high enough to directly initiate a detonation wave in the center core reactants.

Construction, testing, and analysis of the coaxial split flow PDE are planned and should be carried out to completion. Optical ports should be implemented to allow for advanced optical diagnostics.

THIS PAGE INTENTIONALLY LEFT BLANK

APPENDIX A: COMPONENT DRAWINGS



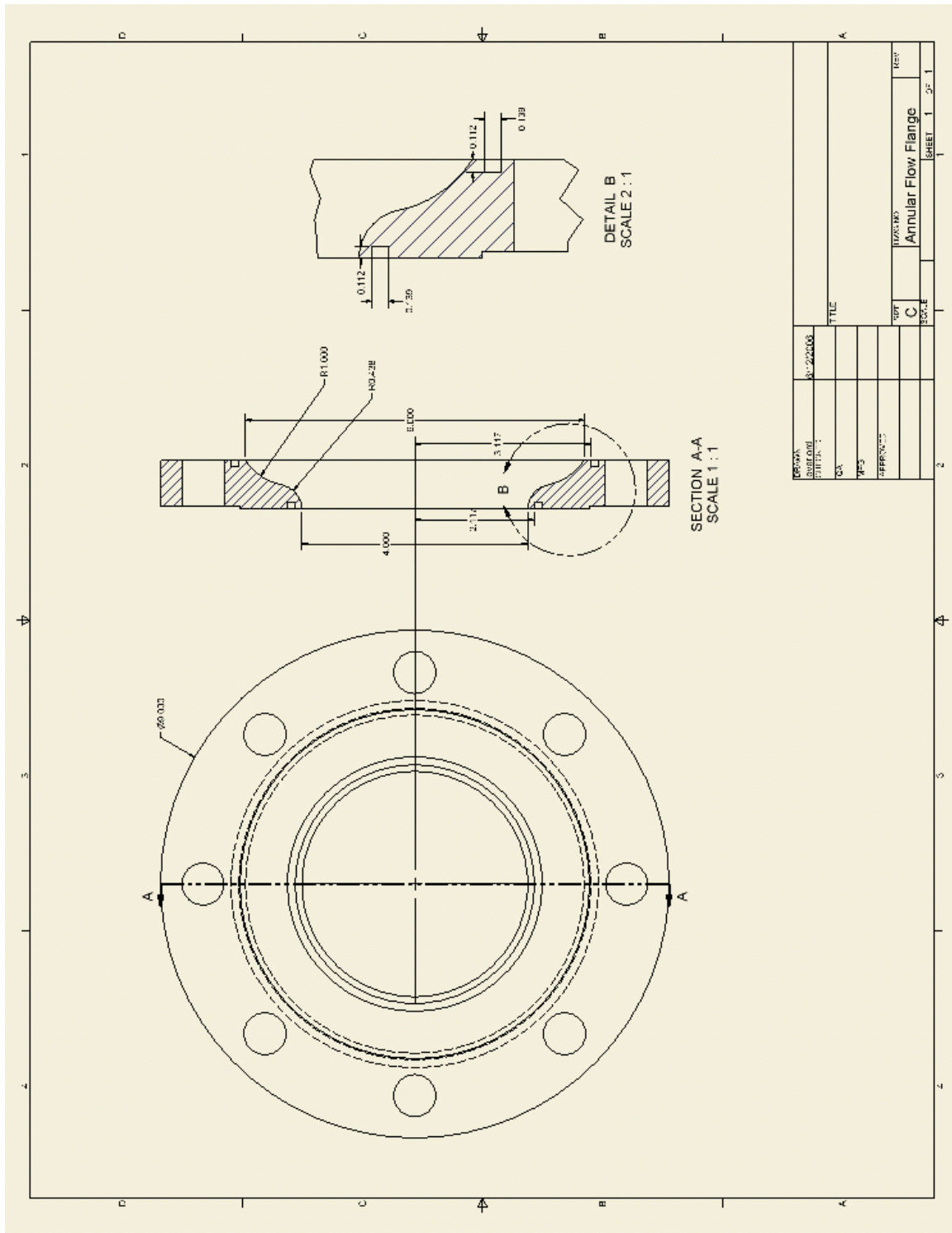


Figure 25. Inlet Flow Flange

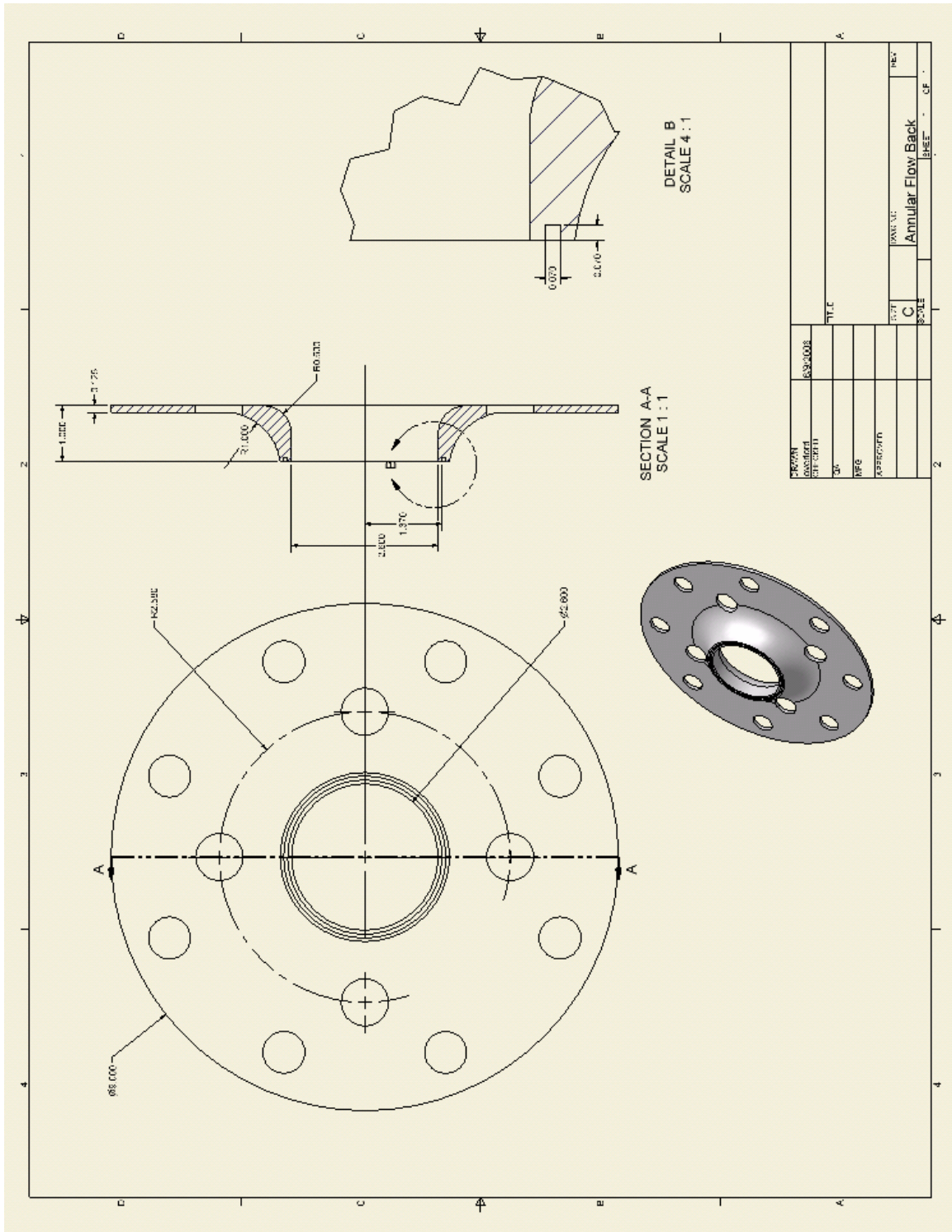


Figure 26. Inlet Flow Backing Plate

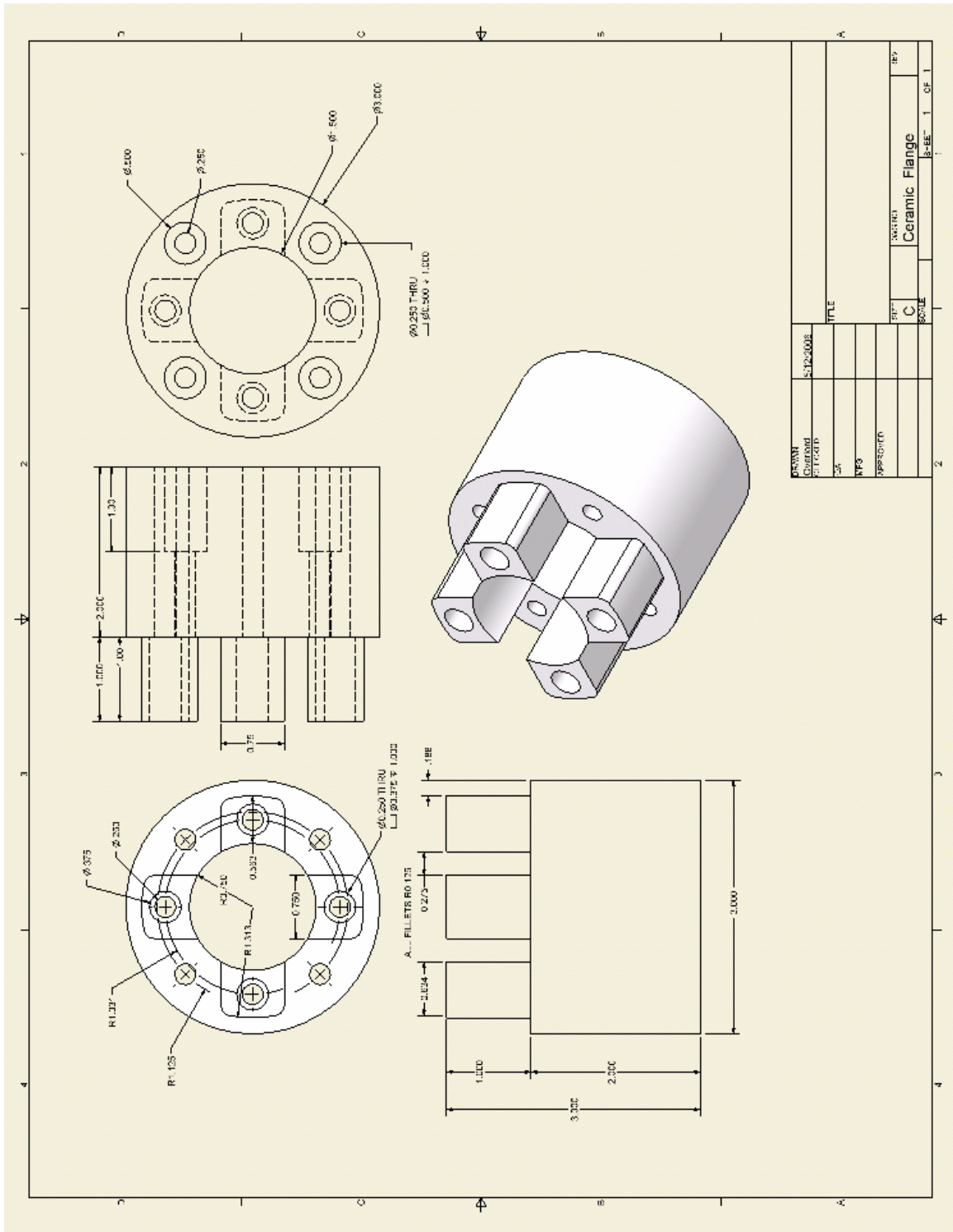


Figure 27. Head Flange Insulator

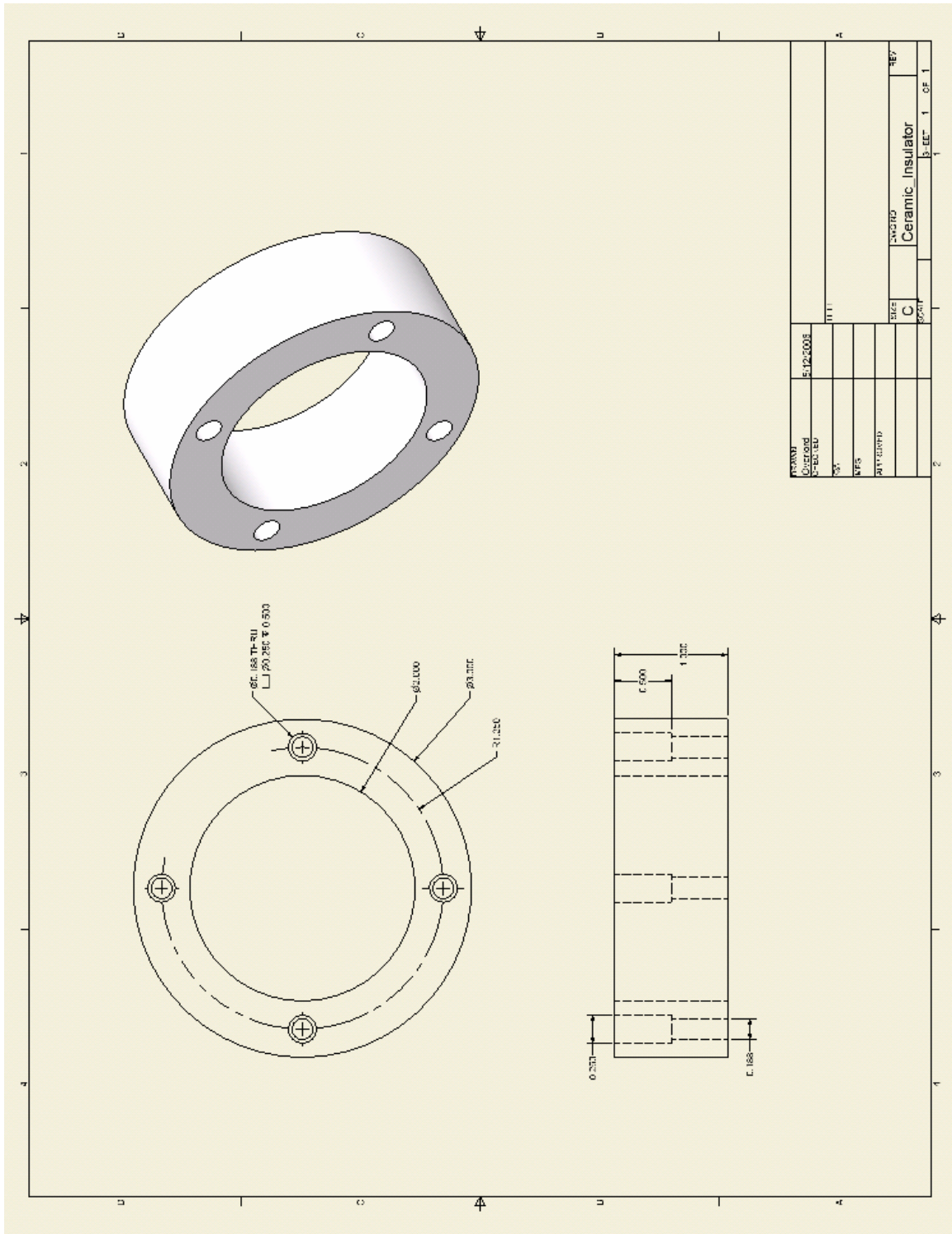


Figure 28. Aft Insulator

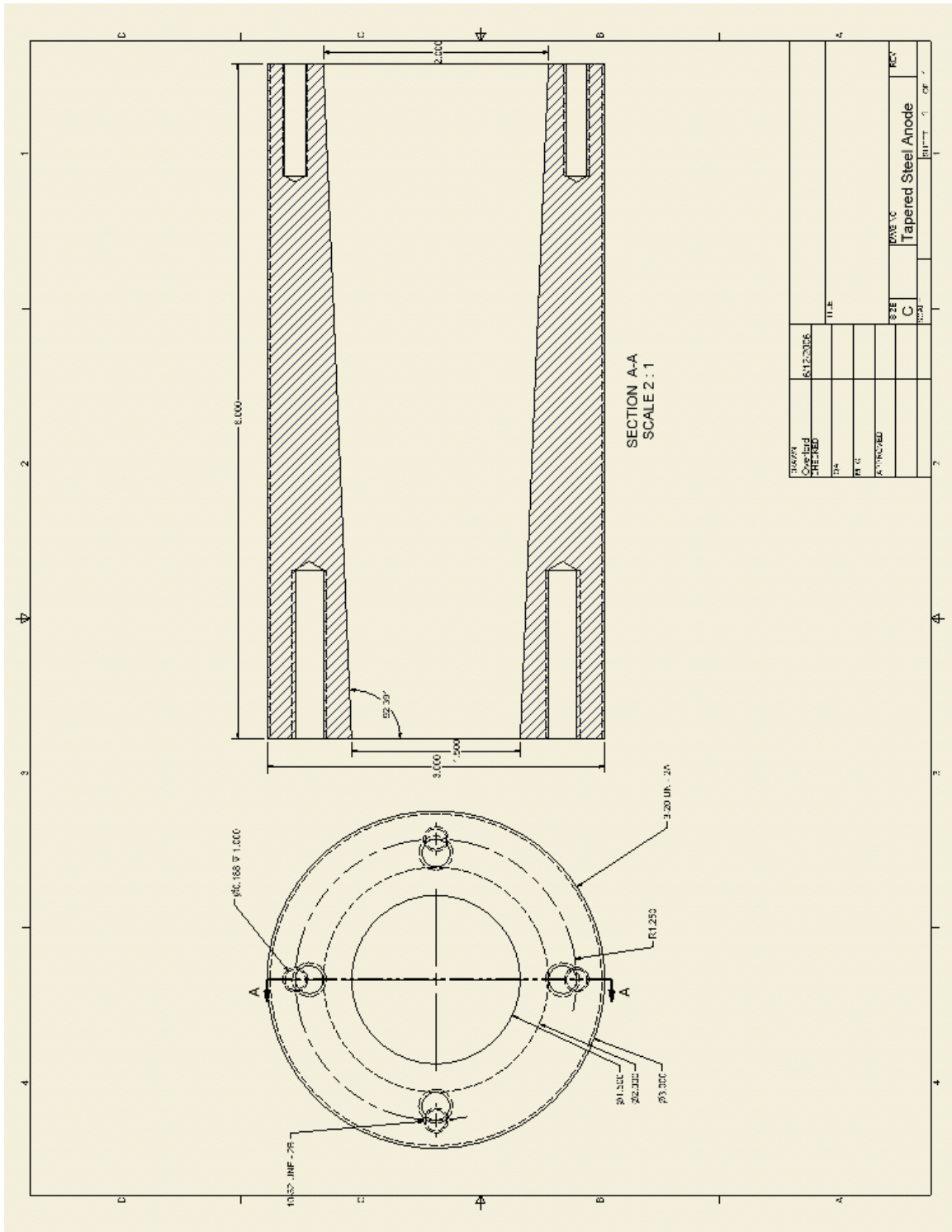


Figure 29. Anode

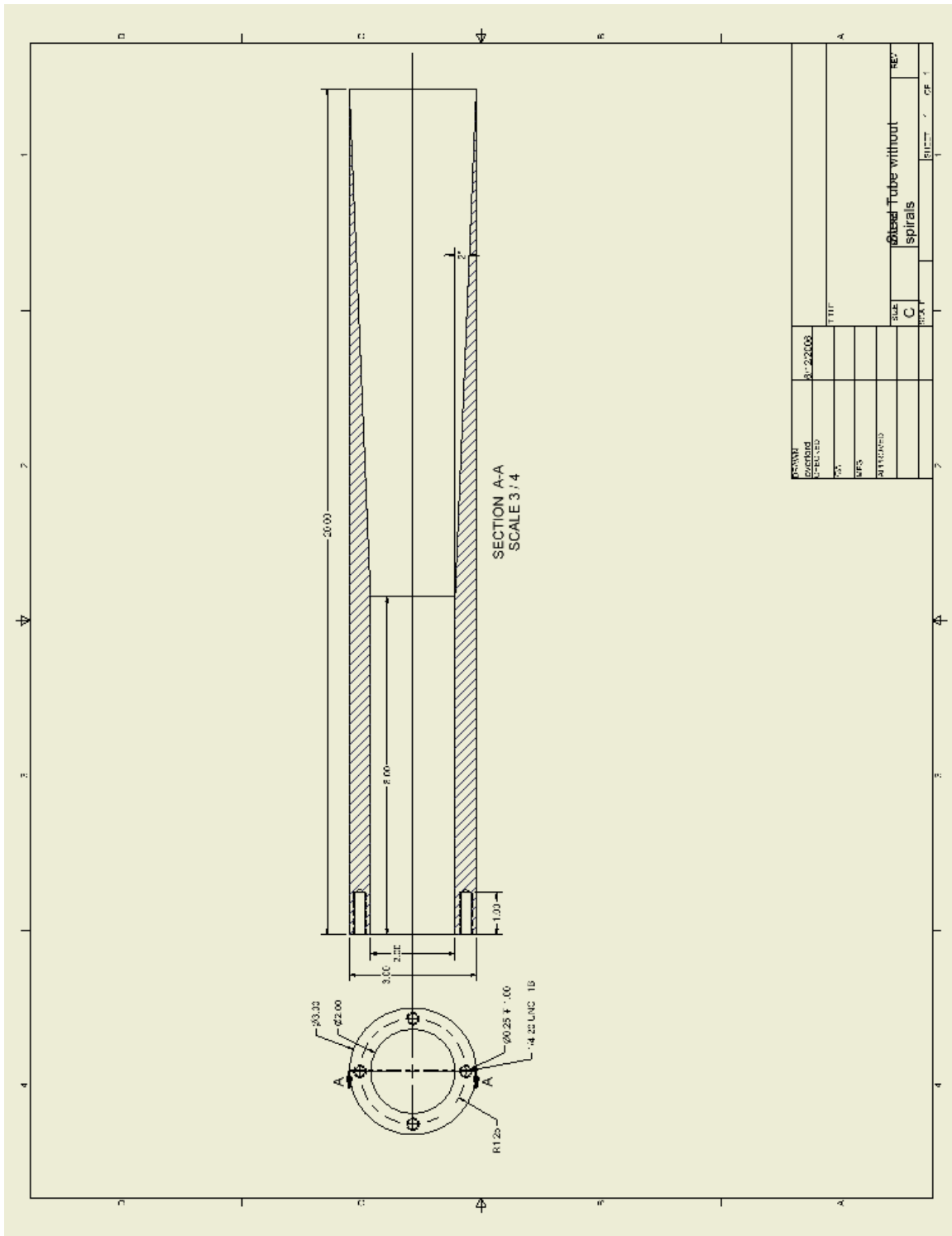


Figure 30. Initiator Tube

LIST OF REFERENCES

1. Glassman, I., *Combustion*, Second Edition, Academic Press, Inc., 1987.
2. van Wingerden, K., Bjerketvedt, D., and Bakke, J. R., "Detonations in Pipes and in the Open," Christian Michelsen Research paper, Bergen, Norway.
3. Channell, Brent, "Evaluation and Selection of an Efficient Fuel/Air Initiation Strategy for Pulse Detonation Engines." Master's Thesis, Naval Postgraduate School, Monterey, California, September, 2005.
4. Fickett, W., and Davis, W. C., *Detonation*, pp. 13-16, University of California Press, 1979.
5. Rodriguez, Joel, "Investigation of Transient Plasma Ignition for a Pulse Detonation Engine." Master's Thesis, Naval Postgraduate School, Monterey, California, March, 2005.
6. Kuo, K. K., *Principles of Combustion*, pp. 231-273, John Wiley & Sons, Inc., 1986.
7. Gundersen, M., "Transient Plasma Ignition – Non-Thermal Plasma Actuator", <http://www.usc.edu/dept/ee/Gundersen/ignition.htm#Transient>, May 2006.
8. Bussing, T., and Pappas, G., "An Introduction to Pulse Detonation Engines," AIAA Paper 1994-0263, 32nd AIAA Aerospace Sciences Meeting and Exhibit, Reno, Nevada, 10-13 January 1994.
9. Shepherd, J. E., Jackson, S. I., "Detonation Initiation via Imploding Shock Waves." AIAA Paper 2004-3919, 40th Joint Propulsion Conference and Exhibit, 11-14 July 2004.
10. Holthaus, John, "Computational Investigation of the Internal Flow Path and Wave Dynamics of Pulse Detonation Engine Operation." Master's Thesis, Naval Postgraduate School, Monterey, California, June 2006.
11. Robbins, Tad, "Fuel Injection Strategy for a Next Generation Pulse Detonation Engine." Master's Thesis, Naval Postgraduate School, Monterey, California, June 2006.

12. <http://www.pr.afrl.af.mil/mar/2005/nov2005.pdf>, June 2006.

INITIAL DISTRIBUTION LIST

1. Defense Technical Information Center
Ft. Belvoir, Virginia
2. Dudley Knox Library
Naval Postgraduate School
Monterey, California
3. Dr. Gabriel Roy
Office of Naval Research
Arlington, VA
4. Professor Jose Sinibaldi
Department of Mechanical and Astronautical Engineering
Naval Postgraduate School
Monterey, CA
5. Professor Christopher Brophy
Department of Mechanical and Astronautical Engineering
Naval Postgraduate School
Monterey, CA
6. Dr. Martin Gundersen
University of Southern California
Los Angeles, CA
7. ENS Philip Hall
Naval Postgraduate School
Monterey, CA